EUROPEAN ORGANIZATION FOR NUCLEAR RESEARCH (CERN)

CERN-EP-2021-216
LHCb-PAPER-2021-034
November 2, 2021

Study of B_c^+ decays to charmonia and three light hadrons

LHCb collaboration[†]

Abstract

Using proton-proton collision data, corresponding to an integrated luminosity of $9\,\text{fb}^{-1}$ collected with the LHCb detector, seven decay modes of the B_c^+ meson into a J/ψ or $\psi(2S)$ meson and three charged hadrons, kaons or pions, are studied. The decays $B_c^+ \to (\psi(2S) \to J/\psi\,\pi^+\pi^-)\pi^+$, $B_c^+ \to \psi(2S)\pi^+\pi^-\pi^+$, $B_c^+ \to J/\psi\,K^+\pi^-\pi^+$ and $B_c^+ \to J/\psi\,K^+K^-K^+$ are observed for the first time, and evidence for the $B_c^+ \to \psi(2S)K^+K^-\pi^+$ decay is found, where J/ψ and $\psi(2S)$ mesons are reconstructed in their dimuon decay modes. The ratios of branching fractions between the different B_c^+ decays are reported as well as the fractions of the decays proceeding via intermediate resonances. The results largely support the factorisation approach used for a theoretical description of the studied decays.

Submitted to JHEP

[†]Authors are listed at the end of this paper.

1 Introduction

The B_c^+ mesons are unique because they contain two different heavy-flavour quarks, charm and beauty. The ground state has a rich set of weak-decay modes since either of the heavy quarks can decay with the other behaving as a spectator quark, or both quarks can annihilate via a virtual W^+ boson. Studies of B_c^+ decay channels and measurements of their branching fractions improve the understanding of models describing strong interactions and test various effective models. Experiments at the Large Hadron Collider (LHC) have opened a new era for B_c^+ meson investigations. The high b-quark production cross-section at the LHC enables the LHCb experiment to study the production, decays and other properties of the B_c^+ meson [1–21].

Although the B_c^+ meson was discovered in 1998 by the CDF collaboration [22, 23], only two $B_c^+ \to \psi 3h^\pm$ decay channels,[1] where the symbol ψ denotes a J/ψ or a $\psi(2S)$ meson and $h^\pm$ stands for a charged kaon or pion, were previously observed by the LHCb collaboration [1,6]. The decays of B_c^+ mesons into charmonium and light hadrons are expected to be well described by the factorisation approach [24, 25]. In this scheme, the $B_c^+ \to \psi 3h^\pm$ decay is characterised by the form factors of the $B_c^+ \to \psi W^+$ transition and the universal spectral function for the virtual W^+ boson fragmenting into light hadrons [26]. The ratios of branching fractions of various $B_c^+ \to \psi 3h^\pm$ decays, based on this theoretical approach are predicted in Refs. [27, 28]. A measurement of the branching fractions of the exclusive B_c^+ meson decays into the final states consisting of charmonium and light hadrons allows for precise tests of the factorisation approach.

In this paper a study of the B_c^+ meson decaying into seven final states, namely the Cabibbo-favoured $B_c^+ \to J/\psi \pi^+\pi^-\pi^+$, $B_c^+ \to \psi(2S)\pi^+\pi^-\pi^+$, $B_c^+ \to J/\psi K^+K^-\pi^+$, $B_c^+ \to \psi(2S)K^+K^-\pi^+$, $B_c^+ \to (\psi(2S) \to J/\psi \pi^+\pi^-)\pi^+$ decays, and the Cabibbo-suppressed $B_c^+ \to J/\psi K^+\pi^-\pi^+$ and $B_c^+ \to J/\psi K^+K^-K^+$ decays, is reported. The analysis is based on proton-proton (pp) collision data, corresponding to an integrated luminosity of 9 fb^{-1} collected with the LHCb detector between 2011 and 2018 at centre-of-mass energies of 7, 8, and 13 TeV. The J/ψ and $\psi(2S)$ mesons are reconstructed from their decay into two muons and the $\psi(2S) \to J/\psi \pi^+\pi^-$ channel is used for the $B_c^+ \to \psi(2S)\pi^+$ decay. The ratios of branching fractions for the decay channels under study are presented.

2 Detector and simulation

The LHCb detector [29, 30] is a single-arm forward spectrometer covering the pseudorapidity range $2 < \eta < 5$, designed for the study of particles containing b or c quarks. The detector includes a high-precision tracking system consisting of a silicon-strip vertex detector surrounding the pp interaction region [31], a large-area silicon-strip detector located upstream of a dipole magnet with a bending power of about 4 Tm, and three stations of silicon-strip detectors and straw drift tubes [32, 33] placed downstream of the magnet. The tracking system provides a measurement of the momentum of charged particles with a relative uncertainty that varies from 0.5% at low momentum to 1.0% at 200 GeV/c. The momentum scale is calibrated using samples of $J/\psi \to \mu^+\mu^-$ and $B^+ \to J/\psi K^+$ decays collected concurrently with the data sample used for this analysis [34, 35]. The relative accuracy of this procedure is estimated to be 3×10^{-4} using samples of other fully re-

[1] Inclusion of charge-conjugate states is implied throughout the paper.

constructed b hadrons, Υ and K^0_S mesons. The minimum distance between a track and a primary pp-collision vertex (PV), the impact parameter, is measured with a resolution of $(15 + 29/p_T)\,\mu$m, where p_T is the component of the momentum transverse to the beam, in GeV/c. Different types of charged hadrons are distinguished using information from two ring-imaging Cherenkov detectors (RICH) [36]. Photons, electrons and hadrons are identified by a calorimeter system consisting of scintillating-pad and preshower detectors, an electromagnetic and a hadronic calorimeter. Muons are identified by a system composed of alternating layers of iron and multiwire proportional chambers [37].

The online event selection is performed by a trigger [38], which consists of a hardware stage, based on information from the calorimeter and muon systems, followed by a software stage, which performs a full event reconstruction. The hardware trigger selects muon candidates with high transverse momentum or dimuon candidates with a high value of the product of the individual muon p_T. In the software trigger, two oppositely-charged muons are required to form a good-quality vertex that is significantly displaced from any PV, and to have a dimuon mass exceeding $2.7\,\text{GeV}/c^2$.

Simulated events are used to describe the signal and to compute efficiencies needed to determine the branching fraction ratios. In the simulation, pp collisions are generated using Pythia [39] with a specific LHCb configuration [40]. Decays of unstable particles are described by the EvtGen package [41], in which final-state radiation is generated using Photos [42]. The simulated decays of $B_c^+ \to J/\psi\,\pi^+\pi^-\pi^+$ and $B_c^+ \to \psi(2S)\pi^+\pi^-\pi^+$ are produced via an intermediate $a_1(1260)^+$ state, followed by $a_1(1260)^+ \to \rho^0\pi^+$ decay, using the phenomenological model by Berezhnoy, Likhoded, and Luchinsky [26, 28, 43] and referred to as BLL model hereafter. The simulated decays of $B_c^+ \to J/\psi\,K^+\pi^-\pi^+$, $B_c^+ \to J/\psi\,K^+K^-\pi^+$, and $B_c^+ \to \psi(2S)K^+K^-\pi^+$ include intermediate K^{*0} and $\overline{K}^{*0}$ states in the $K^+\pi^-$ and $K^-\pi^+$ systems, respectively. In the $B_c^+ \to J/\psi\,K^+K^-K^+$ decay several excited K^{*+} states are included, with fractions in accordance to the observations described in Refs. [44, 45]. All simulated $B_c^+ \to \psi 3h^\pm$ decays are further corrected to reproduce the $\pi^+\pi^-$, $K^+\pi^-$, $K^-\pi^+$, and K^+K^- mass distributions observed in data. The interaction of the generated particles with the detector, and its response, are implemented using the Geant4 toolkit [46] as described in Ref. [47]. To account for imperfections in the simulation of charged-particle reconstruction, the track-reconstruction efficiency determined from simulation is corrected using calibration samples [48].

3 Event selection

Candidate $B_c^+ \to \psi 3h^\pm$ decays are reconstructed using dimuon decays of the J/ψ and $\psi(2S)$ mesons. The criteria largely follow that described in Refs. [6, 7]. The selection starts from reconstructed charged tracks of good quality that are inconsistent with being produced in a pp interaction vertex. Muon, pion and kaon candidates are identified by combining information from the RICH, calorimeter and muon detectors [49]. The muon candidates are required to have a transverse momentum larger than $550\,\text{MeV}/c$. Pairs of oppositely-charged muons consistent with originating from a common vertex are combined to form $J/\psi \to \mu^+\mu^-$ and $\psi(2S) \to \mu^+\mu^-$ candidates. The reconstructed mass of the $\mu^+\mu^-$ pair is required to be in the range $3.0 < m_{\mu^+\mu^-} < 3.2$ GeV/c^2 and $3.60 < m_{\mu^+\mu^-} < 3.73$ GeV/c^2 for the J/ψ and $\psi(2S)$ candidates, respectively. The kaon candidates are required to have a transverse momentum larger than $800\,\text{MeV}/c$ for the $B_c^+ \to J/\psi\,K^+\pi^-\pi^+$ candidates and

500 MeV/c for the other decay modes. The transverse momentum of pion candidates is required to be greater than 500 MeV/c in the $\mathrm{B_c^+} \to \mathrm{J/\psi\,K^+\pi^-\pi^+}$ channel and 400 MeV/c in the other decay modes. For efficient particle identification, kaons and pions are required to have a momentum between 3.2 GeV/c and 150 GeV/c. To reduce combinatorial background, only tracks that are inconsistent with originating from any reconstructed PV in the event are considered.

To form the $\mathrm{B_c^+}$ candidates, the selected ψ candidates are combined with three charged tracks identified as kaons or pions, requiring a good-quality reconstructed vertex. Each $\mathrm{B_c^+}$ candidate is associated with the PV that yields the smallest χ^2_{IP}, where χ^2_{IP} is defined as the difference in the vertex-fit χ^2 of a given PV reconstructed with and without the particle under consideration. To improve the mass resolution for the $\mathrm{B_c^+}$ candidates, a kinematic fit [50] is performed. This fit constrains the mass of the $\mu^+\mu^-$ pair to the known mass of the J/ψ or ψ(2S) meson [51] and constrains the $\mathrm{B_c^+}$ candidate to originate from its associated PV. A requirement on the quality of this fit is applied to further suppress combinatorial background. Such requirement also reduces contributions from the $\mathrm{B_c^+}$ decays with the intermediate weakly-decayed hadron, such as the $\mathrm{B_c^+} \to \mathrm{J/\psi\,(D_s^+ \to 3h^\pm)}$, $\mathrm{B_c^+} \to \mathrm{J/\psi\,(D^0 \to h^+h^-)K^+}$, or $\mathrm{B_c^+} \to \mathrm{\left(B^0_{(s)} \to J/\psi\,h^+h^-\right)h^+}$ decays [3, 5, 15].

The measured decay time of the $\mathrm{B_c^+}$ candidate, calculated with respect to the associated PV, is required to be greater than 175 μm/c for the $\mathrm{B_c^+ \to J/\psi\,\pi^+\pi^-\pi^+}$, $\mathrm{B_c^+ \to \psi(2S)\pi^+\pi^-\pi^+}$, and $\mathrm{B_c^+ \to J/\psi\,K^+\pi^-\pi^+}$ candidates, and 125 μm/c for other decay modes. This requirement suppresses random combinations of candidates, which include tracks originating from the PV. The mass of selected $\mathrm{B_c^+}$ candidates is required to be between 6.15 GeV/c^2 and 6.45 GeV/c^2.

To suppress $\psi\mathrm{3h^\pm}$ combinations with intermediate $\mathrm{B_s^0}$, $\mathrm{B^0}$, $\mathrm{D_s^+}$, and $\mathrm{D^0}$ mesons, a veto is applied on the mass of the corresponding two- or three-body combinations, namely $\psi\mathrm{K^+K^-}$, $\psi\mathrm{K^\mp\pi^\pm}$, $\mathrm{K^+K^-\pi^+}$, and $\mathrm{K^-\pi^+}$. All candidates having any of these masses within a range of approximately $\pm 3\sigma_m$ around the known masses of the intermediate particles [51], where σ_m stands for the mass resolution, are rejected. For the $\mathrm{B_c^+ \to J/\psi\,\pi^+\pi^-\pi^+}$ decay the contribution from the $\mathrm{B_c^+ \to (\psi(2S) \to J/\psi\,\pi^+\pi^-)\,\pi^+}$ decays is removed by rejecting candidates with the $\mathrm{J/\psi\,\pi^+\pi^-}$ mass within the range $3.67 < m_{\mathrm{J/\psi\,\pi^+\pi^-}} < 3.70$ GeV/c^2. For the $\mathrm{B_c^+ \to \psi(2S)K^+K^-\pi^+}$ decay the mass of the $\mathrm{K^-\pi^+}$ system is required to be between 0.74 GeV/c^2 and 1.04 GeV/c^2, consistent with originating from a $\overline{\mathrm{K}}^{*0}$ meson.

Mass distributions for selected $\mathrm{B_c^+ \to J/\psi\,\pi^+\pi^-\pi^+}$, $\mathrm{B_c^+ \to \psi(2S)\pi^+\pi^-\pi^+}$, $\mathrm{B_c^+ \to J/\psi\,K^+K^-\pi^+}$, $\mathrm{B_c^+ \to \psi(2S)K^+K^-\pi^+}$, $\mathrm{B_c^+ \to J/\psi\,K^+\pi^-\pi^+}$ and $\mathrm{B_c^+ \to J/\psi\,K^+K^-K^+}$ candidates are shown in Fig. 1. Figure 2 (left) shows the mass distribution for selected $\mathrm{B_c^+ \to (\psi(2S) \to J/\psi\,\pi^+\pi^-)\,\pi^+}$ candidates, while the corresponding mass distribution for $\mathrm{\psi(2S) \to J/\psi\,\pi^+\pi^-}$ candidates is shown in Fig. 2 (right).

4 Signal yields

The yields for the $\mathrm{B_c^+ \to \psi 3h^\pm}$ decays are determined using a simultaneous extended unbinned maximum-likelihood fit to the six mass distributions of selected $\mathrm{B_c^+ \to J/\psi\,\pi^+\pi^-\pi^+}$, $\mathrm{B_c^+ \to \psi(2S)\pi^+\pi^-\pi^+}$, $\mathrm{B_c^+ \to J/\psi\,K^+\pi^-\pi^+}$, $\mathrm{B_c^+ \to J/\psi\,K^+K^-\pi^+}$, $\mathrm{B_c^+ \to \psi(2S)K^+K^-\pi^+}$ and $\mathrm{B_c^+ \to J/\psi\,K^+K^-K^+}$ candidates; and a two-dimensional distribution of the $\mathrm{J/\psi\,\pi^+\pi^-\pi^+}$ mass, $m_{\mathrm{J/\psi\,\pi^+\pi^-\pi^+}}$, versus $\mathrm{J/\psi\,\pi^+\pi^-}$ mass, $m_{\mathrm{J/\psi\,\pi^+\pi^-}}$, for the $\mathrm{B_c^+ \to (\psi(2S) \to J/\psi\,\pi^+\pi^-)\pi^+}$ candidates. To improve the resolution on

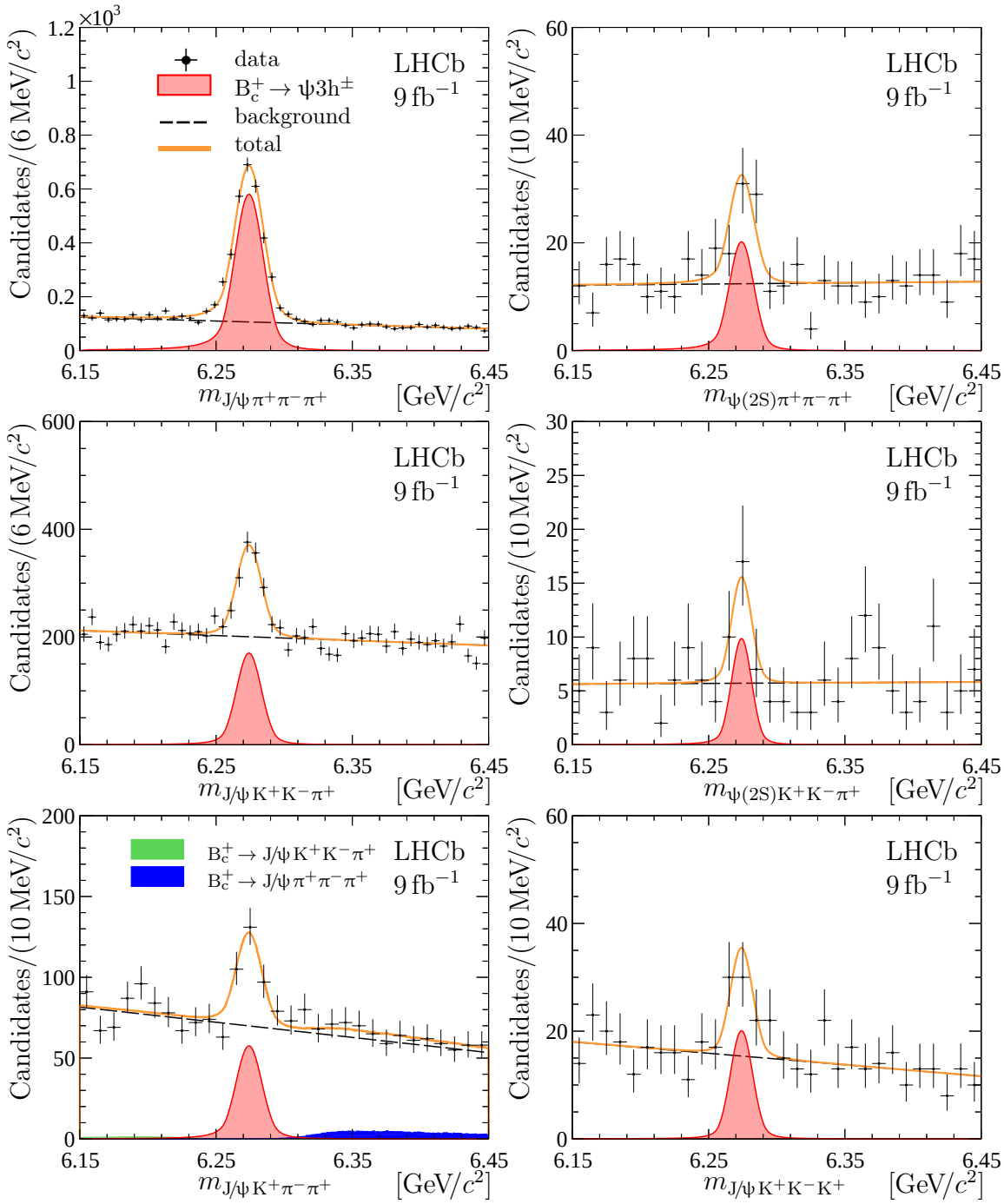

Figure 1: Mass distributions for selected $B_c^+ \to \psi 3h^\pm$ candidates. Projections of a fit, described in the text, are overlaid.

the $J/\psi\pi^+\pi^-$ mass for the $B_c^+ \to (\psi(2S) \to J/\psi\pi^+\pi^-)\pi^+$ candidates and to eliminate a small correlation between $m_{J/\psi\pi^+\pi^-\pi^+}$ and $m_{J/\psi\pi^+\pi^-}$, following Refs. [52,53] the $m_{J/\psi\pi^+\pi^-}$ variable is computed [50] by constraining the mass of the B_c^+ candidate to its known value [51]. For each B_c^+ mass distribution the one-dimensional fit function consists of two components:

1. signal $B_c^+ \to \psi 3h^\pm$ decays parameterised by a modified Gaussian function with power-law tails on both sides of the distribution [54, 55]. The tail parameters are fixed to the values obtained from simulation;

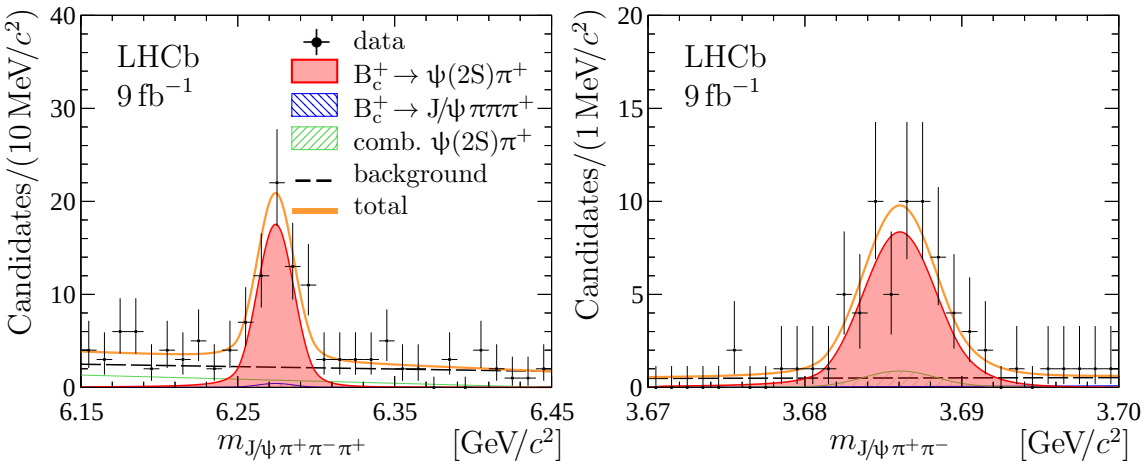

Figure 2: Distributions of the (left) $J/\psi\pi^+\pi^-\pi^+$ and (right) $J/\psi\pi^+\pi^-$ masses for selected $B_c^+ \to (\psi(2S) \to J/\psi\pi^+\pi^-)\pi^+$ candidates. Projections of a fit, described in the text, are overlaid. The right plot corresponds to the mass range $6.24 < m_{J/\psi\pi^+\pi^-\pi^+} < 6.31\,\text{GeV}/c^2$.

2. random $\psi 3h^\pm$ combinations, modelled by a first-order polynomial function.

The two-dimensional fit function for the $B_c^+ \to (\psi(2S) \to J/\psi\pi^+\pi^-)\pi^+$ channel is defined as a sum of four components:

1. signal $B_c^+ \to (\psi(2S) \to J/\psi\pi^+\pi^-)\pi^+$ decays parameterised as a product of B_c^+ and $\psi(2S)$ signal functions modelled by a modified Gaussian function with power-law tails on both sides of the distribution [54, 55]. The tail parameters are fixed to the values obtained from simulation;

2. contributions from the decays $B_c^+ \to (J/\psi\pi^+\pi^-)_{\text{NR}}\pi^+$ without proceeding through a narrow intermediate $\psi(2S)$ state, parameterised as a product of the B_c^+ signal function and a linear function of $m_{J/\psi\pi^+\pi^-}$;

3. random combinations of $\psi(2S)$ and π^+ candidates, parameterised as a product of the $\psi(2S)$ signal template as obtained from simulation and a linear function of $m_{J/\psi\pi^+\pi^-\pi^+}$, multiplied by the two-body phase-space function [56];

4. random $J/\psi\pi^+\pi^-\pi^+$ combinations, described by a two-dimensional positive-definite first-order polynomial function.

For the Cabibbo-suppressed channel $B_c^+ \to J/\psi K^+\pi^-\pi^+$, components describing feed-down contributions from the Cabibbo-favoured $B_c^+ \to J/\psi K^+K^-\pi^+$ and $B_c^+ \to J/\psi\pi^+\pi^-\pi^+$ decays, where the kaon is misidentified as a pion or vice versa, are added into the fit function. The shapes for these contributions are taken from simulation, and their yields are constrained to the expected number of misidentified events.

For all B_c^+ signal functions, the peak-position parameter is shared between all decays and allowed to vary in the fit. The mass-resolution parameters used in the B_c^+ and $\psi(2S)$ signal functions are fixed to the values determined from simulation, and corrected by scale factors, $s_{B_c^+}$ and $s_{\psi(2S)}$, to account for a discrepancy in the mass resolution between data and simulation [52, 53, 57]. These factors are allowed to vary in the fit, and the factor $s_{B_c^+}$ is shared for all decay modes. The factor $s_{\psi(2S)}$ and the peak-position

Table 1: Parameters of interest from the simultaneous unbinned extended maximum-likelihood fit. The uncertainties are statistical only. For previously unobserved decay modes, the last column shows the statistical significance estimated using pseudoexperiments in units of standard deviations.

Decay	Yield	$\mathcal{S}$ $[\sigma]$
$\mathrm{B_c^+} \to \mathrm{J/\psi}\,\pi^+\pi^-\pi^+$	2750 ± 69	
$\mathrm{B_c^+} \to \mathrm{J/\psi}\,\mathrm{K^+K^-}\pi^+$	686 ± 48	
$\mathrm{B_c^+} \to \mathrm{J/\psi}\,\mathrm{K^+K^-K^+}$	43 ± 10	5.2
$\mathrm{B_c^+} \to \mathrm{J/\psi}\,\mathrm{K^+}\pi^-\pi^+$	148 ± 22	7.8
$\mathrm{B_c^+} \to \psi(2\mathrm{S})\pi^+\pi^-\pi^+$	49 ± 11	5.8
$\mathrm{B_c^+} \to \psi(2\mathrm{S})\mathrm{K^+K^-}\pi^+$	19 ± 6	3.7
$\mathrm{B_c^+} \to (\psi(2\mathrm{S}) \to \mathrm{J/\psi}\,\pi^+\pi^-)\pi^+$	54 ± 9	11.8
Parameter	**Value**	
$m_{\mathrm{B_c^+}}$ $[\mathrm{MeV}/c^2]$	6274.14 ± 0.26	
$m_{\psi(2\mathrm{S})}$ $[\mathrm{MeV}/c^2]$	3686.05 ± 0.01	

parameter for the $\psi(2S)$ signal component are constrained to the values from a previous LHCb study [52]. The mass distributions together with projections of the fit are shown in Fig. 1 for $\mathrm{B_c^+} \to \mathrm{J/\psi}\,\pi^+\pi^-\pi^+$, $\mathrm{B_c^+} \to \psi(2\mathrm{S})\pi^+\pi^-\pi^+$, $\mathrm{B_c^+} \to \mathrm{J/\psi}\,\mathrm{K^+K^-}\pi^+$, $\mathrm{B_c^+} \to \psi(2\mathrm{S})\mathrm{K^+K^-}\pi^+$, $\mathrm{B_c^+} \to \mathrm{J/\psi}\,\mathrm{K^+}\pi^-\pi^+$ and $\mathrm{B_c^+} \to \mathrm{J/\psi}\,\mathrm{K^+K^-K^+}$ candidates and Fig. 2 for the $\mathrm{B_c^+} \to (\psi(2\mathrm{S}) \to \mathrm{J/\psi}\,\pi^+\pi^-)\,\pi^+$ candidates. The fit parameters of interest with statistical significance of the observed signals are summarised in Table 1. The resolution correction factors are found to be $s_{\mathrm{B_c^+}} = 1.096 \pm 0.029$ and $s_{\psi(2\mathrm{S})} = 1.048 \pm 0.004$.

The statistical significance for previously unobserved decay modes is estimated with a large number of pseudoexperiments produced according to the background distribution observed in data. These results amount to the first observation of the decays $\mathrm{B_c^+} \to \psi(2\mathrm{S})\pi^+\pi^-\pi^+$, $\mathrm{B_c^+} \to \mathrm{J/\psi}\,\mathrm{K^+}\pi^-\pi^+$ and $\mathrm{B_c^+} \to \mathrm{J/\psi}\,\mathrm{K^+K^-K^+}$ decays, and the first evidence for the $\mathrm{B_c^+} \to \psi(2\mathrm{S})\mathrm{K^+K^-}\pi^+$ decay. The decay $\mathrm{B_c^+} \to \psi(2\mathrm{S})\pi^+$ is confirmed using the $\psi(2\mathrm{S}) \to \mathrm{J/\psi}\,\pi^+\pi^-$ mode.

5 Resonance structure

The $\pi^+\pi^-\pi^+$ and $\pi^+\pi^-$ mass distributions from the $\mathrm{B_c^+} \to \mathrm{J/\psi}\,\pi^+\pi^-\pi^+$ decays were previously studied in Ref. [1] and were shown to be compatible with originating from a $\mathrm{B_c^+} \to \mathrm{J/\psi}\,\mathrm{a_1}(1260)^+$, followed by an $\mathrm{a_1}(1260)^+ \to \rho^0\pi^+$ decay [26, 43]. The background-subtracted $\pi^+\pi^-\pi^+$ and $\pi^+\pi^-$ distribution for the $\mathrm{B_c^+} \to \mathrm{J/\psi}\,\pi^+\pi^-\pi^+$ candidates are shown in Fig. 3, where the *sPlot* technique is used for background subtraction [58], using the $\mathrm{J/\psi}\,\pi^+\pi^-\pi^+$ mass as a discriminating variable.

The $\pi^+\pi^-\pi^+$ mass distribution agrees well with the BLL model expectations [26, 28, 43]. The $\pi^+\pi^-$ mass distribution exhibits a clear peak from the ρ^0 resonance and a structure near $m_{\pi^+\pi^-} \sim 1.3\,\mathrm{GeV}/c^2$, that can be due to contributions from the decays of the wide $\mathrm{a_1}(1260)^+$ resonance via $\mathrm{f_2}(1270)$, $\mathrm{f_0}(1370)$ or $\rho(1450)$ mesons [60], jointly referred to as R in the following. Unbinned maximum-likelihood fits to the $\pi^+\pi^-$ mass

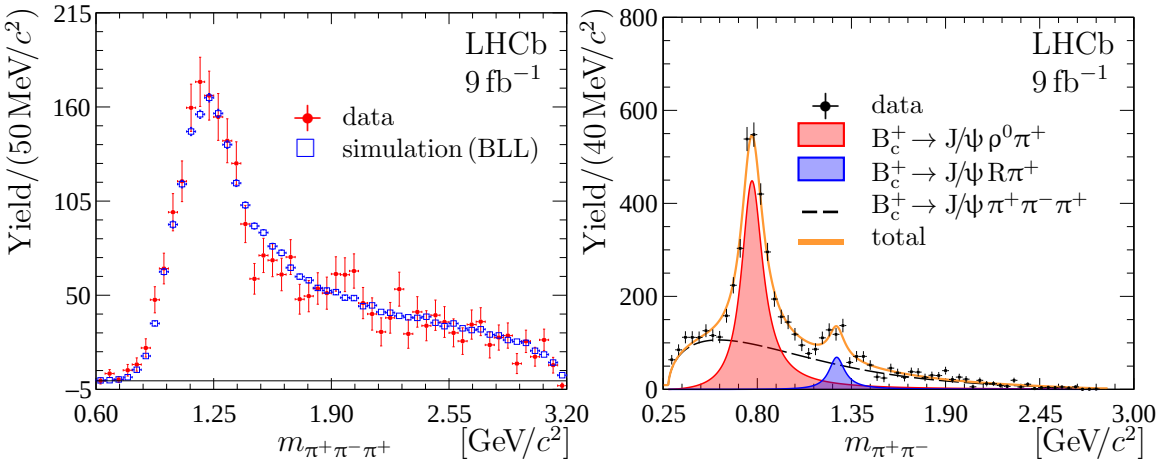

Figure 3: Background-subtracted (left) $\pi^+\pi^-\pi^+$ and (right) $\pi^+\pi^-$ mass distributions for selected $B_c^+ \to J/\psi\,\pi^+\pi^-\pi^+$ candidates. In the left plot the expectation from simulation for the $B_c^+ \to J/\psi\,a_1(1260)^+$ decays with BLL model [26, 28, 43] is overlaid.

Table 2: Results for parameters from the fit to the background-subtracted $\pi^+\pi^-$ mass spectrum from the $B_c^+ \to J/\psi\,\pi^+\pi^-\pi^+$ decays. The last row shows the statistical significance for the R structure estimated using Wilks' theorem [59].

Parameter		Value
$f_{\rho^0}^{B_c^+\to J/\psi\pi^+\pi^-\pi^+}$	[%]	88.1 ± 3.0
$f_R^{B_c^+\to J/\psi\pi^+\pi^-\pi^+}$	[%]	10.4 ± 1.4
m_R	[MeV/c^2]	1265 ± 10
Γ_R	[MeV]	110 ± 21
$\mathcal{S}_R$	[σ]	8

distribution are performed with functions that contain three terms: a component corresponding to the decay via the ρ^0 resonance; a component corresponding to the decays via S-, P-, or D-wave $\pi^+\pi^-$ resonances, and a component corresponding to B_c^+ meson decays into the $J/\psi\,\pi^+\pi^-\pi^+$ final state without resonances in the $\pi^+\pi^-$ system. The resonance components are parameterised with relativistic P- and S-wave Breit–Wigner functions with Blatt–Weisskopf form factors with a meson radius of 3.5 GeV^{-1} [61].[2] The non-resonant component is parameterised with a product of the phase-space function describing a two-body system out of the four-body final state [56] and a positive second-order polynomial function, that accounts for the decay dynamics via the intermediate $a_1(1260)^+$ state. The ρ^0 peak position and the width are constrained to their known values [51] using Gaussian constraints, while parameters for the R structure are free to vary in the fit.

The fractions $f_{\rho^0}^{B_c^+\to J/\psi\pi^+\pi^-\pi^+}$ and $f_R^{B_c^+\to J/\psi\pi^+\pi^-\pi^+}$ of the B_c^+ meson decays into

[2]Blatt–Weisskopf form factors with meson radius of 3.5 GeV^{-1} are used for all subsequent fits with relativistic Breit–Wigner functions, unless stated otherwise.

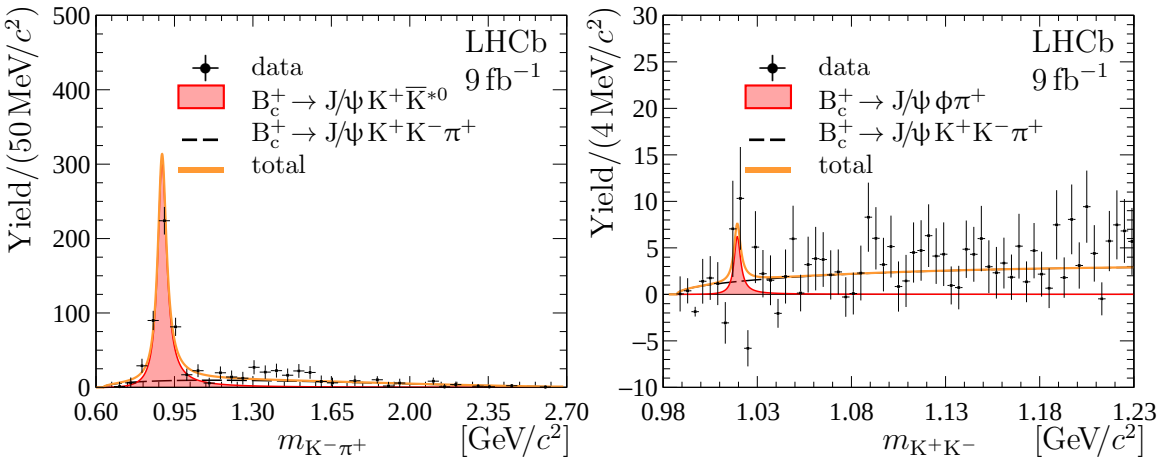

Figure 4: Background-subtracted (left) $K^-\pi^+$ and (right) K^+K^- mass distributions for selected $B_c^+ \to J/\psi K^+K^-\pi^+$ candidates. The K^+K^- mass spectrum is fitted in the full accessible K^+K^- mass region, $m_{K^+K^-} < 2.923\,\text{GeV}/c^2$. For better visibility, only a low-mass part of the spectrum is shown.

the $J/\psi\pi^+\pi^-\pi^+$ final state via the intermediate ρ^0 and R resonances, as well as the Breit–Wigner mass and width for the R structure, m_R and Γ_R, are shown in Table 2. The results for fractions, mass and width of the resonance are stable with respect to the choice of the orbital momentum used for the Breit–Wigner function: f_{ρ^0} and f_R change by 0.002, m_R and Γ_R change by respectively $2\,\text{MeV}/c^2$ and 3 MeV, when the orbital momentum varies from S-wave to D-wave. The statistical significance for the structure is estimated using Wilks' theorem [59] and is found to be 8 standard deviations. The obtained Breit–Wigner mass and width of the structure are consistent with those for the $f_0(1370)$ state [51]. The yield relative to the yield of decays via the ρ^0 resonance, $(11.8 \pm 1.6)\,\%$, agrees with that obtained by the CLEO collaboration from a Dalitz analysis of the $a_1(1260)^+ \to \pi^+\pi^0\pi^0$ decay [60], and is much larger than those for the $f_2(1270)$ and $\rho(1450)$ states. It allows interpretation of the R structure as the $f_0(1370)$ resonance, however alternative interpretations such as the $f_2(1270)$ or $\rho(1450)$ state are also possible.

In Ref. [6] it has been demonstrated that a large fraction of the decays of the B_c^+ mesons into the $J/\psi K^+K^-\pi^+$ final state proceeds via an intermediate $\overline{K}^{*0}$ meson, while no evidence for Okubo–Zweig–Iizuka-suppressed (OZI) decays [62–64] via intermediate ϕ mesons is found. Figure 4 shows the background-subtracted $K^-\pi^+$ and K^+K^- mass distributions for the selected $B_c^+ \to J/\psi K^+K^-\pi^+$ candidates. Unbinned maximum-likelihood fits to these distributions are performed with functions consisting of two terms: a component corresponding to decays via intermediate $\overline{K}^{*0} \to K^-\pi^+$ or $\phi \to K^+K^-$ decays and a component without resonances in $K^-\pi^+$ or K^+K^- systems. The former is parameterised with a relativistic P-wave Breit–Wigner function, while the latter is parameterised with a phase-space function describing a two-body system in a four-body final state [56]. Masses and widths of the $\overline{K}^{*0}$ and ϕ resonances are allowed to vary in the fit and are Gaussian constrained to their known values [51]. Results of the fits are overlaid in Fig. 4. The fractions of the B_c^+ meson decays into the $J/\psi K^+K^-\pi^+$ final state via intermediate

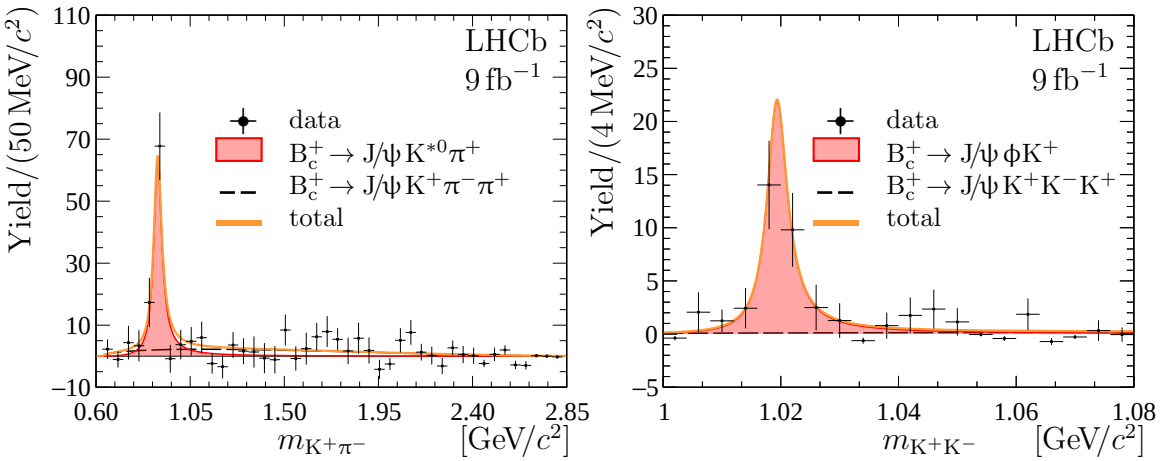

Figure 5: Background-subtracted mass distributions of (left) $K^+\pi^-$ pairs for the selected $B_c^+ \to J/\psi K^+\pi^-\pi^+$ candidates and (right) K^+K^- combinations for the selected $B_c^+ \to J/\psi K^+K^-K^+$ candidates. The K^+K^- mass spectrum is fitted in the full accessible K^+K^- mass region, $m_{K^+K^-} < 2.2\,\text{GeV}/c^2$. For better visibility, only a low-mass part of the spectrum is shown.

$\overline{K}^{*0}$ and ϕ resonances are found to be

$$f_{\overline{K}^{*0}}^{B_c^+ \to J/\psi K^+K^-\pi^+} = (64.5 \pm 4.7)\,\%\,,$$
$$f_{\phi}^{B_c^+ \to J/\psi K^+K^-\pi^+} = \left(1.6\,^{+0.7}_{-0.6}\right)\,\%\,,$$

respectively, confirming the previous observations [6]. The upper limit at 90 (95)% confidence level (CL) on the fraction $f_{\phi}^{B_c^+ \to J/\psi K^+K^-\pi^+}$ is set as

$$f_{\phi}^{B_c^+ \to J/\psi K^+K^-\pi^+} < 3.9\,(4.5)\%\,.$$

The background-subtracted $K^+\pi^-$ and K^+K^- mass distributions for selected Cabibbo-suppressed $B_c^+ \to J/\psi K^+\pi^-\pi^+$ and $B_c^+ \to J/\psi K^+K^-K^+$ candidates are shown in Fig. 5. Fits to these distributions with two-component functions similar to those described above are performed and results of the fits are overlaid in Fig. 5. For B_c^+ decays into the $J/\psi K^+\pi^-\pi^+$ final state a large fraction proceeds via a K^{*0} meson,

$$f_{K^{*0}}^{B_c^+ \to J/\psi K^+\pi^-\pi^+} = (61.3 \pm 5.0)\,\%$$

and for B_c^+ decays into the $J/\psi K^+K^-K^+$ final state a dominant fraction proceeds via a ϕ meson,

$$f_{\phi}^{B_c^+ \to J/\psi K^+K^-K^+} = (90 \pm 19)\,\%\,.$$

All uncertainties for these resonance fractions are statistical only.

6 Ratios of branching fractions

Six ratios of branching fractions are reported in this paper,

$$\mathcal{R}_{J/\psi K^+K^-\pi^+}^{J/\psi K^+K^-K^+} \equiv \frac{\mathcal{B}(B_c^+ \to J/\psi K^+K^-K^+)}{\mathcal{B}(B_c^+ \to J/\psi K^+K^-\pi^+)}\,, \tag{1a}$$

$$\mathcal{R}^{\mathrm{J/\psi K^+\pi^-\pi^+}}_{\mathrm{J/\psi K^+K^-\pi^+}} \equiv \frac{\mathcal{B}(\mathrm{B_c^+ \to J/\psi K^+\pi^-\pi^+})}{\mathcal{B}(\mathrm{B_c^+ \to J/\psi K^+K^-\pi^+})}\,, \tag{1b}$$

$$\mathcal{R}^{\mathrm{\psi(2S)K^+K^-\pi^+}}_{\mathrm{J/\psi K^+K^-\pi^+}} \equiv \frac{\mathcal{B}(\mathrm{B_c^+ \to \psi(2S)K^+K^-\pi^+}) \times \mathcal{B}(\mathrm{\psi(2S) \to \mu^+\mu^-})}{\mathcal{B}(\mathrm{B_c^+ \to J/\psi K^+K^-\pi^+}) \times \mathcal{B}(\mathrm{J/\psi \to \mu^+\mu^-})}\,, \tag{1c}$$

$$\mathcal{R}^{\mathrm{\psi(2S)\pi^+\pi^-\pi^+}}_{\mathrm{J/\psi \pi^+\pi^-\pi^+}} \equiv \frac{\mathcal{B}(\mathrm{B_c^+ \to \psi(2S)\pi^+\pi^-\pi^+}) \times \mathcal{B}(\mathrm{\psi(2S) \to \mu^+\mu^-})}{\mathcal{B}(\mathrm{B_c^+ \to J/\psi \pi^+\pi^-\pi^+}) \times \mathcal{B}(\mathrm{J/\psi \to \mu^+\mu^-})}\,, \tag{1d}$$

$$\mathcal{R}^{\mathrm{\psi(2S)\pi^+}}_{\mathrm{J/\psi \pi^+\pi^-\pi^+}} \equiv \frac{\mathcal{B}(\mathrm{B_c^+ \to \psi(2S)\pi^+}) \times \mathcal{B}(\mathrm{\psi(2S) \to J/\psi \pi^+\pi^-})}{\mathcal{B}(\mathrm{B_c^+ \to J/\psi \pi^+\pi^-\pi^+})}\,, \tag{1e}$$

$$\mathcal{R}^{\mathrm{J/\psi K^+K^-\pi^+}}_{\mathrm{J/\psi \pi^+\pi^-\pi^+}} \equiv \frac{\mathcal{B}(\mathrm{B_c^+ \to J/\psi K^+K^-\pi^+})}{\mathcal{B}(\mathrm{B_c^+ \to J/\psi \pi^+\pi^-\pi^+})}\,, \tag{1f}$$

where decays are paired to give the largest cancellation of systematic uncertainties. Each ratio of branching fractions for $\mathrm{B_c^+ \to X}$ and $\mathrm{B_c^+ \to Y}$ decay modes, $\mathcal{R}^{\mathrm{X}}_{\mathrm{Y}}$, is calculated as

$$\mathcal{R}^{\mathrm{X}}_{\mathrm{Y}} = \frac{N_{\mathrm{X}}}{N_{\mathrm{Y}}} \times \frac{\varepsilon_{\mathrm{Y}}}{\varepsilon_{\mathrm{X}}}\,, \tag{2}$$

where N is the signal yield reported in Table 1 and ε denotes the efficiency of the corresponding decay. The efficiency is defined as the product of geometric acceptance, reconstruction, selection, hadron identification and trigger efficiencies. All of these contributions, except that of the hadron-identification efficiency, are determined using simulated samples, corrected as described above. The hadron-identification efficiency is calculated from single-track hadron identification efficiencies for kaons and pions, determined from large calibration samples of $\mathrm{D^{*+} \to (D^0 \to K^-\pi^+)\,\pi^+}$, $\mathrm{K^0_S \to \pi^+\pi^-}$ and $\mathrm{D_s^+ \to (\phi \to K^+K^-)\,\pi^+}$ decays [36, 65].

The measured ratios of branching fractions are

$$\begin{aligned}
\mathcal{R}^{\mathrm{J/\psi K^+K^-K^+}}_{\mathrm{J/\psi K^+K^-\pi^+}} &= (7.0 \pm 1.8) \times 10^{-2}\,,\\
\mathcal{R}^{\mathrm{J/\psi K^+\pi^-\pi^+}}_{\mathrm{J/\psi K^+K^-\pi^+}} &= 0.35 \pm 0.06\,,\\
\mathcal{R}^{\mathrm{\psi(2S)K^+K^-\pi^+}}_{\mathrm{J/\psi K^+K^-\pi^+}} &= (3.7 \pm 1.2) \times 10^{-2}\,,\\
\mathcal{R}^{\mathrm{\psi(2S)\pi^+\pi^-\pi^+}}_{\mathrm{J/\psi \pi^+\pi^-\pi^+}} &= (1.9 \pm 0.4) \times 10^{-2}\,,\\
\mathcal{R}^{\mathrm{\psi(2S)\pi^+}}_{\mathrm{J/\psi \pi^+\pi^-\pi^+}} &= (3.5 \pm 0.6) \times 10^{-2}\,,\\
\mathcal{R}^{\mathrm{J/\psi K^+K^-\pi^+}}_{\mathrm{J/\psi \pi^+\pi^-\pi^+}} &= 0.185 \pm 0.013\,,
\end{aligned}$$

where uncertainties are statistical only and correlation coefficients are listed in Table A.1. Systematic uncertainties are discussed in Sec. 7.

7 Systematic uncertainties

The decay channels under study have similar kinematics and topologies, therefore a large part of systematic uncertainties cancels in the branching fraction ratios $\mathcal{R}^{\mathrm{X}}_{\mathrm{Y}}$. The remaining contributions to the systematic uncertainty are summarised in Table 3 and discussed below.

An important source of systematic uncertainty on the ratios arises from the imperfect knowledge of the shapes of signal and background components used in the fits. To estimate

this uncertainty, several alternative models are tested. For the B_c^+ and $\psi(2S)$ signal shapes an Apollonios function [66] is employed as an alternative model. The degree of the polynomials used in the fits is increased by one. The systematic uncertainty related to the fit model is estimated by pseudoexperiments with the baseline fit model and fitted with alternative models. Each pseudoexperiment is approximately 100 times larger than the data sample. The maximal deviations in the ratios of the signal yields with respect to the baseline model do not exceed 2.8% for variation of the signal model and 3.7% for variation of background model, and are taken as systematic uncertainties in the ratios $\mathcal{R}_Y^X$.

The simulated $B_c^+ \to \psi 3h^\pm$ decays are corrected to reproduce the two-dimensional $\pi^+\pi^-$, $K^+\pi^-$, $K^-\pi^+$, and K^+K^- mass distributions observed in data. The uncertainty associated with this correction procedure and related to the imperfect knowledge of the B_c^+ decay model is estimated by varying the reference mass distributions within their uncertainties. It causes small changes in the efficiencies and subsequent changes in the ratios $\mathcal{R}_Y^X$, that do not exceed 0.3%. These changes are taken as systematic uncertainties related to the B_c^+ decay model.

An additional uncertainty arises from differences between data and simulation, in particular differences in the reconstruction efficiency of charged-particle tracks. The track-finding efficiencies obtained from simulation are corrected using data calibration samples [48]. The uncertainties related to the correction factors, together with the uncertainty in the hadron-identification efficiency due to the finite size of the calibration samples [36, 65], are propagated to the ratio of total efficiencies using pseudoexperiments. The obtained systematic uncertainty for the $\mathcal{R}_Y^X$ ratios do not exceed 1.6%.

The systematic uncertainty related to the trigger efficiency is estimated by comparing the ratios of trigger efficiencies in data and simulation using large samples of the $B^+ \to J/\psi K^+$ and $B^+ \to \psi(2S)K^+$ decays [67]. Another source of uncertainty is a potential disagreement between data and simulation in the estimation of efficiencies, due to possible effects not considered above. This is studied by varying the selection criteria in ranges that lead up to a $\pm 20\%$ change in the measured signal yields. For this study, the high yield $B_c^+ \to J/\psi \pi^+\pi^-\pi^+$ data sample is used. The resulting difference between the efficiencies estimated using data and simulation does not exceed 3.0%, which is taken as a systematic uncertainty for the ratios $\mathcal{R}_Y^X$. The last systematic uncertainty considered for the ratios $\mathcal{R}_Y^X$ is due to the finite size of the simulated samples and it varies between 0.6% and 2.1%.

Systematic uncertainties for the fractions of decays via resonances are estimated by variation of the fit models. In particular, the meson radii are varied between 1.5 and $5\,\mathrm{GeV}^{-1}$, the degree of polynomial functions is varied from one to three and, for $B_c^+ \to J/\psi \pi^+\pi^-\pi^+$ decays, the Gounaris–Sakurai function [68] is used for the ρ^0 meson parameterisation. For each alternative model the fit fraction is determined and the maximal difference in the fractions with respect to the default fit model is taken as a corresponding systematic uncertainty. The systematic uncertainties for the fractions are summarised in Table 4. For the fraction $f_\phi^{B_c^+ \to J/\psi K^+K^-\pi^+}$, the upper limits are estimated for each alternative model, and the largest value is taken. The upper limit at 90 (95)% CL that accounts for the systematic uncertainty is $f_\phi^{B_c^+ \to J/\psi K^+K^-\pi^+} < 4.2\,(4.8)\%$.

Table 3: Ranges of relative systematic uncertainties for the ratios of branching fractions $\mathcal{R}^{X}_{Y}$. The total systematic uncertainty is the quadratic sum of individual contributions.

Source	Uncertainty [%]
Fit model	
Signal shape	$< 0.1 - 2.8$
Background shape	$0.2 - 3.7$
B_c^+ decay model	$< 0.1 - 0.3$
Efficiency corrections	$< 0.1 - 1.6$
Trigger efficiency	1.1
Data-simulation difference	3.0
Size of simulated sample	$0.6 - 2.1$
Total	$3.3 - 5.6$

Table 4: Systematic uncertainties for the fractions of the decays via resonances.

Fraction	Uncertainty [%]
$f_{\rho^0}^{B_c^+ \to J/\psi \pi^+\pi^-\pi^+}$	$^{+12.0}_{-0.3}$
$f_{R}^{B_c^+ \to J/\psi \pi^+\pi^-\pi^+}$	$^{+8.0}_{-1.2}$
$f_{\overline{K}^{*0}}^{B_c^+ \to J/\psi K^+K^-\pi^+}$	$^{+3.9}_{-4.8}$
$f_{K^{*0}}^{B_c^+ \to J/\psi K^+\pi^-\pi^+}$	$^{+7.7}_{-0.3}$
$f_{\phi}^{B_c^+ \to J/\psi K^+K^-K^+}$	$^{+5.0}_{-7.0}$

8 Results and summary

The $B_c^+ \to \psi 3h^{\pm}$ decays are studied using proton-proton collision data, corresponding to an integrated luminosity of $9\,fb^{-1}$, collected with the LHCb detector. The first observation of the decays $B_c^+ \to \psi(2S)\pi^+\pi^-\pi^+$, $B_c^+ \to J/\psi K^+\pi^-\pi^+$ and $B_c^+ \to J/\psi K^+K^-K^+$ is reported. The decay $B_c^+ \to \psi(2S)\pi^+$ is confirmed using $\psi(2S) \to J/\psi \pi^+\pi^-$ mode and the first evidence for the $B_c^+ \to \psi(2S)K^+K^-\pi^+$ decay is obtained with a significance of 3.7 standard deviations.

The three-pion mass distribution for the $B_c^+ \to J/\psi \pi^+\pi^-\pi^+$ decays is found to be consistent with a BLL model for the $B_c^+ \to J/\psi\, a_1(1260)^+$ decay based on the factorisation approach [26, 28, 43], in agreement with previous studies [1]. The presence of the intermediate axial $a_1(1260)^+$ meson in this decay is further supported by a large fraction of the $B_c^+ \to J/\psi \pi^+\pi^-\pi^+$ decays proceeding via the intermediate ρ^0 resonance

$$f_{\rho^0}^{B_c^+ \to J/\psi \pi^+\pi^-\pi^+} = \left(88.1 \pm 3.0\, ^{+12.0}_{-0.3}\right)\%\,,$$

and the observation of a structure in the $\pi^+\pi^-$ mass spectrum, consistent with the $a_1(1260)^+ \to (f_0(1370) \to \pi^+\pi^-)\,\pi^+$ decay. The fraction of the $B_c^+ \to J/\psi \pi^+\pi^-\pi^+$ de-

Table 5: Comparison of the measured ratios $\mathcal{R}_{\rm Y}^{\rm X}$ with their theoretical predictions or derivations from previous measurements.

Ratio	Value	Prediction, measurement	Reference
$\mathcal{R}^{\psi(2S)K^+K^-\pi^+}_{\psi(2S)\pi^+\pi^-\pi^+}$	$0.37 \pm 0.15 \pm 0.01$	0.16	BLL [27, 28]
$\mathcal{R}^{J/\psi K^+\pi^-\pi^+}_{J/\psi K^+K^-\pi^+}$	$0.35 \pm 0.06 \pm 0.01$	0.37	BLL [27]
$\mathcal{R}^{J/\psi K^+\pi^-\pi^+}_{J/\psi \pi^+\pi^-\pi^+}$	$(6.4 \pm 1.0 \pm 0.2) \times 10^{-2}$	7.7×10^{-2}	BLL [27]
$\mathcal{R}^{J/\psi K^+K^-\pi^+}_{J/\psi \pi^+\pi^-\pi^+}$	$0.185 \pm 0.013 \pm 0.006$	0.21	BLL [27, 28]
$\mathcal{R}^{\psi(2S)\pi^+}_{J/\psi K^+K^-\pi^+}$	$0.19 \pm 0.03 \pm 0.01$	0.18 ± 0.04	LHCb [6, 11]
$\mathcal{R}^{\psi(2S)\pi^+}_{J/\psi \pi^+\pi^-\pi^+}$	$(3.5 \pm 0.6 \pm 0.2) \times 10^{-2}$	$(3.9 \pm 0.9) \times 10^{-2}$	LHCb [1, 11]
$\mathcal{R}^{J/\psi K^+K^-\pi^+}_{J/\psi \pi^+\pi^-\pi^+}$	$0.185 \pm 0.013 \pm 0.006$	0.22 ± 0.06	LHCb [1, 6]

cays proceeding via this intermediate state is found to be

$$f_{\rm R}^{B_c^+ \to J/\psi \pi^+\pi^-\pi^+} = \left(10.4 \pm 1.4 ^{+8.0}_{-1.2}\right) \%\,,$$

which agrees with the value of $(7.40 \pm 2.71 \pm 1.26)\,\%$, obtained by the CLEO collaboration for the fraction of the $a_1(1260)^+ \to \pi^+\pi^0\pi^0$ decays proceeding via intermediate $f_0(1370)$ state [60].

The fraction of the $B_c^+ \to J/\psi\, K^+K^-\pi^+$ decays proceeding via intermediate $\overline{K}^{*0}$ state is measured to be

$$f_{\overline{K}^{*0}}^{B_c^+ \to J/\psi K^+K^-\pi^+} = \left(64.5 \pm 4.7 ^{+3.9}_{-4.8}\right) \%\,,$$

while no evidence for OZI-suppressed decays $B_c^+ \to J/\psi\, (\phi \to K^+K^-)\, \pi^+$ is found and the upper limit at 90 (95)% CL of the corresponding fraction of the $B_c^+ \to J/\psi\, K^+K^-\pi^+$ decays proceeding via intermediate ϕ meson is set to be

$$f_{\phi}^{B_c^+ \to J/\psi K^+K^-\pi^+} < 4.2\,(4.8)\%\,.$$

Both results are in agreement with the previous study by the LHCb collaboration [6]. For the $B_c^+ \to J/\psi\, K^+\pi^-\pi^+$ and $B_c^+ \to J/\psi\, K^+K^-K^+$ decays large fractions of decays via intermediate K^{*0} and ϕ resonances, respectively, are found

$$\begin{aligned} f_{K^{*0}}^{B_c^+ \to J/\psi K^+\pi^-\pi^+} &= \left(61.3 \pm 5.0 ^{+7.7}_{-0.3}\right) \%\,, \\ f_{\phi}^{B_c^+ \to J/\psi K^+K^-K^+} &= \left(90 \pm 19 ^{+5}_{-7}\right) \%\,. \end{aligned}$$

The six ratios of branching fractions are measured as

$$\begin{aligned} \mathcal{R}^{J/\psi K^+K^-K^+}_{J/\psi K^+K^-\pi^+} &= (7.0 \pm 1.8 \pm 0.2) \times 10^{-2}\,, \\ \mathcal{R}^{J/\psi K^+\pi^-\pi^+}_{J/\psi K^+K^-\pi^+} &= 0.35 \pm 0.06 \pm 0.01\,, \\ \mathcal{R}^{\psi(2S)K^+K^-\pi^+}_{J/\psi K^+K^-\pi^+} &= (3.7 \pm 1.2 \pm 0.1) \times 10^{-2}\,, \end{aligned}$$

Table 6: Comparison of the measured ratios of branching fractions for the Cabibbo-suppressed and Cabibbo-favoured decays with the ratios of branching fraction for similar decays of B_c^+, B^+, B^0 and B_s^0 mesons [14, 51, 69–71].

	Value [10^{-2}]	Reference
$\mathcal{R}^{J/\psi K^+K^-K^+}_{J/\psi K^+K^-\pi^+}$	$7.0 \pm 1.8 \pm 0.2$	This paper
$\mathcal{R}^{J/\psi K^+\pi^-\pi^+}_{J/\psi \pi^+\pi^-\pi^+}$	$6.4 \pm 1.0 \pm 0.2$	This paper
$\frac{\mathcal{B}(B_c^+ \to J/\psi K^+)}{\mathcal{B}(B_c^+ \to J/\psi \pi^+)}$	7.9 ± 0.8	[14]
$\frac{\mathcal{B}(B^+ \to \overline{D}{}^0 K^+\pi^-\pi^+)}{\mathcal{B}(B^+ \to \overline{D}{}^0\pi^+\pi^-\pi^+)}$	9.3 ± 5.1	[51, 69]
$\frac{\mathcal{B}(B^0 \to D^- K^+\pi^-\pi^+)}{\mathcal{B}(B^0 \to D^-\pi^+\pi^-\pi^+)}$	5.8 ± 1.5	[51, 69]
$\frac{\mathcal{B}(B^0 \to D^{*-} K^+\pi^-\pi^+)}{\mathcal{B}(B^0 \to D^{*-}\pi^+\pi^-\pi^+)}$	6.5 ± 0.6	[51, 70]
$\frac{\mathcal{B}(B_s^0 \to D_s^- K^+\pi^-\pi^+)}{\mathcal{B}(B_s^0 \to D_s^-\pi^+\pi^-\pi^+)}$	5.2 ± 1.3	[51, 71]

$$
\begin{aligned}
\mathcal{R}^{\psi(2S)\pi^+\pi^-\pi^+}_{J/\psi\pi^+\pi^-\pi^+} &= (1.9 \pm 0.4 \pm 0.1) \times 10^{-2} \\
\mathcal{R}^{\psi(2S)\pi^+}_{J/\psi\pi^+\pi^-\pi^+} &= (3.5 \pm 0.6 \pm 0.2) \times 10^{-2}\,, \\
\mathcal{R}^{J/\psi K^+K^-\pi^+}_{J/\psi\pi^+\pi^-\pi^+} &= 0.185 \pm 0.013 \pm 0.006\,,
\end{aligned}
$$

where the first uncertainty is statistical and the second systematic. Correlation coefficients for statistical and systematic uncertainties are given in Appendix A. The ratios of branching fractions from this measurement are compared in Table 5 with either theoretical predictions [27, 28] or derivations from previous LHCb measurements [1, 6, 11].

The ratio of branching fractions for the B_c^+ decays via $\psi(2S)$ and J/ψ mesons, $\mathcal{R}^{\psi(2S)K^+K^-\pi^+}_{J/\psi K^+K^-\pi^+}$, agrees with the known ratio of branching fractions for the $B_c^+ \to \psi(2S)\pi^+$ and $B_c^+ \to J/\psi\pi^+$ decays $\mathcal{R}^{\psi(2S)\pi^+}_{J/\psi\pi^+} = (3.54 \pm 0.43) \times 10^{-2}$ [11], however the similar ratio for the $B_c^+ \to \psi(2S)\pi^+\pi^-\pi^+$ and $B_c^+ \to J/\psi\pi^+\pi^-\pi^+$ channels, $\mathcal{R}^{\psi(2S)\pi^+\pi^-\pi^+}_{J/\psi\pi^+\pi^-\pi^+}$, is in tension, at 2.8 standard deviations, with the measured ratio $\mathcal{R}^{\psi(2S)\pi^+}_{J/\psi\pi^+}$ [11]. The ratio $\mathcal{R}^{J/\psi K^+K^-K^+}_{J/\psi K^+K^-\pi^+}$ of branching fractions for the Cabibbo-suppressed $B_c^+ \to J/\psi K^+K^-K^+$ and Cabibbo-favoured $B_c^+ \to J/\psi K^+K^-\pi^+$ decays agrees within uncertainties with the similar ratio $\mathcal{R}^{J/\psi K^+\pi^-\pi^+}_{J/\psi\pi^+\pi^-\pi^+}$ and the known ratio of branching fractions for the Cabibbo-suppressed $B_c^+ \to J/\psi K^+$ and Cabibbo-favoured $B_c^+ \to J/\psi\pi^+$ decays [14]. The ratios $\mathcal{R}^{J/\psi K^+K^-K^+}_{J/\psi K^+K^-\pi^+}$ and $\mathcal{R}^{J/\psi K^+\pi^-\pi^+}_{J/\psi\pi^+\pi^-\pi^+}$ also agree with the ratios of branching fraction for the multibody decays of B^+, B^0 and B_s^0 mesons, see Table 6. This pattern supports the factorisation hypothesis for the $B_c^+ \to \psi 3h^\pm$ decays.

Acknowledgements

We thank A. K. Likhoded and A. V. Luchinsky for providing us with the code for modelling the $B_c^+ \to \psi 3h^\pm$ decays. We express our gratitude to our colleagues in the CERN accelerator departments for the excellent performance of the LHC. We thank the technical and administrative staff at the LHCb institutes. We acknowledge support from CERN and from the national agencies: CAPES, CNPq, FAPERJ and FINEP (Brazil); MOST and NSFC (China); CNRS/IN2P3 (France); BMBF, DFG and MPG (Germany); INFN (Italy); NWO (Netherlands); MNiSW and NCN (Poland); MEN/IFA (Romania); MSHE (Russia); MICINN (Spain); SNSF and SER (Switzerland); NASU (Ukraine); STFC (United Kingdom); DOE NP and NSF (USA). We acknowledge the computing resources that are provided by CERN, IN2P3 (France), KIT and DESY (Germany), INFN (Italy), SURF (Netherlands), PIC (Spain), GridPP (United Kingdom), RRCKI and Yandex LLC (Russia), CSCS (Switzerland), IFIN-HH (Romania), CBPF (Brazil), PL-GRID (Poland) and NERSC (USA). We are indebted to the communities behind the multiple open-source software packages on which we depend. Individual groups or members have received support from ARC and ARDC (Australia); AvH Foundation (Germany); EPLANET, Marie Skłodowska-Curie Actions and ERC (European Union); A*MIDEX, ANR, IPhU and Labex P2IO, and Région Auvergne-Rhône-Alpes (France); Key Research Program of Frontier Sciences of CAS, CAS PIFI, CAS CCEPP, Fundamental Research Funds for the Central Universities, and Sci. & Tech. Program of Guangzhou (China); RFBR, RSF and Yandex LLC (Russia); GVA, XuntaGal and GENCAT (Spain); the Leverhulme Trust, the Royal Society and UKRI (United Kingdom).

A Correlation matrices

Correlation coefficients for the measured ratios $\mathcal{R}^{\mathrm{X}}_{\mathrm{Y}}$ are shown in Tables A.1 and A.2 for statistical and systematic uncertainties, respectively.

Table A.1: Off-diagonal correlation coefficients ([%]) for statistical uncertainties for the measured ratios $\mathcal{R}^{\mathrm{X}}_{\mathrm{Y}}$.

	$\mathcal{R}^{\mathrm{J/\psi K^+\pi^-\pi^+}}_{\mathrm{J/\psi K^+K^-\pi^+}}$	$\mathcal{R}^{\mathrm{\psi(2S)K^+K^-\pi^+}}_{\mathrm{J/\psi K^+K^-\pi^+}}$	$\mathcal{R}^{\mathrm{\psi(2S)\pi^+\pi^-\pi^+}}_{\mathrm{J/\psi\pi^+\pi^-\pi^+}}$	$\mathcal{R}^{\mathrm{\psi(2S)\pi^+}}_{\mathrm{J/\psi\pi^+\pi^-\pi^+}}$	$\mathcal{R}^{\mathrm{J/\psi K^+K^-\pi^+}}_{\mathrm{J/\psi\pi^+\pi^-\pi^+}}$
$\mathcal{R}^{\mathrm{J/\psi K^+K^-K^+}}_{\mathrm{J/\psi K^+K^-\pi^+}}$	−13	+0	−8	+2	−24
$\mathcal{R}^{\mathrm{J/\psi K^+\pi^-\pi^+}}_{\mathrm{J/\psi K^+K^-\pi^+}}$		+4	−7	+1	−33
$\mathcal{R}^{\mathrm{\psi(2S)K^+K^-\pi^+}}_{\mathrm{J/\psi K^+K^-\pi^+}}$			−1	−3	−15
$\mathcal{R}^{\mathrm{\psi(2S)\pi^+\pi^-\pi^+}}_{\mathrm{J/\psi\pi^+\pi^-\pi^+}}$				−4	+12
$\mathcal{R}^{\mathrm{\psi(2S)\pi^+}}_{\mathrm{J/\psi\pi^+\pi^-\pi^+}}$					+0

Table A.2: Off-diagonal correlation coefficients ([%]) for systematic uncertainties for the measured ratios $\mathcal{R}^{\mathrm{X}}_{\mathrm{Y}}$.

	$\mathcal{R}^{\mathrm{J/\psi K^+\pi^-\pi^+}}_{\mathrm{J/\psi K^+K^-\pi^+}}$	$\mathcal{R}^{\mathrm{\psi(2S)K^+K^-\pi^+}}_{\mathrm{J/\psi K^+K^-\pi^+}}$	$\mathcal{R}^{\mathrm{\psi(2S)\pi^+\pi^-\pi^+}}_{\mathrm{J/\psi\pi^+\pi^-\pi^+}}$	$\mathcal{R}^{\mathrm{\psi(2S)\pi^+}}_{\mathrm{J/\psi\pi^+\pi^-\pi^+}}$	$\mathcal{R}^{\mathrm{J/\psi K^+K^-\pi^+}}_{\mathrm{J/\psi\pi^+\pi^-\pi^+}}$
$\mathcal{R}^{\mathrm{J/\psi K^+K^-K^+}}_{\mathrm{J/\psi K^+K^-\pi^+}}$	+39	+18	+2	−10	−52
$\mathcal{R}^{\mathrm{J/\psi K^+\pi^-\pi^+}}_{\mathrm{J/\psi K^+K^-\pi^+}}$		+27	−7	−4	−60
$\mathcal{R}^{\mathrm{\psi(2S)K^+K^-\pi^+}}_{\mathrm{J/\psi K^+K^-\pi^+}}$			+9	−20	−59
$\mathcal{R}^{\mathrm{\psi(2S)\pi^+\pi^-\pi^+}}_{\mathrm{J/\psi\pi^+\pi^-\pi^+}}$				+27	+30
$\mathcal{R}^{\mathrm{\psi(2S)\pi^+}}_{\mathrm{J/\psi\pi^+\pi^-\pi^+}}$					+37

References

[1] LHCb collaboration, R. Aaij *et al.*, *First observation of the decay* $\mathrm{B_c^+} \to \mathrm{J/\psi}\,\pi^+\pi^-\pi^+$, Phys. Rev. Lett. **108** (2012) 251802, arXiv:1204.0079.

[2] LHCb collaboration, R. Aaij *et al.*, *Observation of the decay* $\mathrm{B_c^+} \to \psi(2S)\pi^+$, Phys. Rev. **D87** (2013) 071103(R), arXiv:1303.1737.

[3] LHCb collaboration, R. Aaij *et al.*, *Observation of* $\mathrm{B_c^+} \to \mathrm{J/\psi\,D_s^+}$ *and* $\mathrm{B_c^+} \to \mathrm{J/\psi\,D_s^{*+}}$ *decays*, Phys. Rev. **D87** (2013) 112012, Erratum ibid. **D89** (2014) 019901(E), arXiv:1304.4530.

[4] LHCb collaboration, R. Aaij *et al.*, *First observation of the decay* $\mathrm{B_c^+} \to \mathrm{J/\psi\,K^+}$, JHEP **09** (2013) 075, arXiv:1306.6723.

[5] LHCb collaboration, R. Aaij *et al.*, *Observation of the decay* $\mathrm{B_c^+} \to \mathrm{B_s^0}\pi^+$, Phys. Rev. Lett. **111** (2013) 181801, arXiv:1308.4544.

[6] LHCb collaboration, R. Aaij *et al.*, *Observation of the decay* $\mathrm{B_c^+} \to \mathrm{J/\psi\,K^+K^-}\pi^+$, JHEP **11** (2013) 094, arXiv:1309.0587.

[7] LHCb collaboration, R. Aaij *et al.*, *Evidence for the decay* $\mathrm{B_c^+} \to \mathrm{J/\psi}\,3\pi^+2\pi^-$, JHEP **05** (2014) 148, arXiv:1404.0287.

[8] LHCb collaboration, R. Aaij *et al.*, *First observation of a baryonic* $\mathrm{B_c^+}$ *decay*, Phys. Rev. Lett. **113** (2014) 152003, arXiv:1408.0971.

[9] LHCb collaboration, R. Aaij *et al.*, *Measurement of* $\mathrm{B_c^+}$ *production in proton-proton collisions at* $\sqrt{s}$ *=8 TeV*, Phys. Rev. Lett. **114** (2015) 132001, arXiv:1411.2943.

[10] LHCb collaboration, R. Aaij *et al.*, *Measurement of the lifetime of the* $\mathrm{B_c^+}$ *meson using the* $\mathrm{B_c^+} \to \mathrm{J/\psi}\,\pi^+$ *decay mode*, Phys. Lett. **B742** (2015) 29, arXiv:1411.6899.

[11] LHCb collaboration, R. Aaij *et al.*, *Measurement of the branching fraction ratio* $\mathcal{B}(\mathrm{B_c^+} \to \psi(2S)\pi^+)/\mathcal{B}(\mathrm{B_c^+} \to \mathrm{J/\psi}\,\pi^+)$, Phys. Rev. **D92** (2015) 072007, arXiv:1507.03516.

[12] LHCb collaboration, R. Aaij *et al.*, *Search for* $\mathrm{B_c^+}$ *decays to the* $\mathrm{p\bar{p}}\pi^+$ *final state*, Phys. Lett. **B759** (2016) 313, arXiv:1603.07037.

[13] LHCb collaboration, R. Aaij *et al.*, *Study of* $\mathrm{B_c^+}$ *decays to the* $\mathrm{K^+K^-}\pi^+$ *final state and evidence for the decay* $\mathrm{B_c^+} \to \chi_{c0}\pi^+$, Phys. Rev. **D94** (2016) 091102(R), arXiv:1607.06134.

[14] LHCb collaboration, R. Aaij *et al.*, *Measurement of the ratio of branching fractions* $\mathcal{B}(\mathrm{B_c^+} \to \mathrm{J/\psi\,K^+})/\mathcal{B}(\mathrm{B_c^+} \to \mathrm{J/\psi}\,\pi^+)$, JHEP **09** (2016) 153, arXiv:1607.06823.

[15] LHCb collaboration, R. Aaij *et al.*, *Observation of* $\mathrm{B_c^+} \to \mathrm{J/\psi\,D^{(*)}K^{(*)}}$ *decays*, Phys. Rev. **D95** (2017) 032005, arXiv:1612.07421.

[16] LHCb collaboration, R. Aaij *et al.*, *Observation of* $\mathrm{B_c^+} \to \mathrm{D^0K^+}$ *decays*, Phys. Rev. Lett. **118** (2017) 111803, arXiv:1701.01856.

[17] LHCb collaboration, R. Aaij *et al.*, *Measurement of the ratio of branching fractions* $\mathcal{B}(\mathrm{B_c^+} \to \mathrm{J/\psi}\,\tau^+\nu_\tau)/\mathcal{B}(\mathrm{B_c^+} \to \mathrm{J/\psi}\,\mu^+\nu_\mu)$, Phys. Rev. Lett. **120** (2018) 121801, arXiv:1711.05623.

[18] LHCb collaboration, R. Aaij *et al.*, *Search for* $\mathrm{B_c^+}$ *decays to two charm mesons*, Nucl. Phys. **B930** (2018) 563, arXiv:1712.04702.

[19] LHCb collaboration, R. Aaij *et al.*, *Measurement of the* $\mathrm{B_c^-}$ *production fraction and asymmetry in 7 and 13 TeV* pp *collisions*, Phys. Rev. **D100** (2019) 112006, arXiv:1910.13404.

[20] LHCb collaboration, R. Aaij *et al.*, *Precision measurement of the* $\mathrm{B_c^+}$ *meson mass*, JHEP **07** (2020) 123, arXiv:2004.08163.

[21] LHCb collaboration, R. Aaij *et al.*, *Updated search for* $\mathrm{B_c^+}$ *decays to two charm mesons*, arXiv:2109.00488, submitted to JHEP.

[22] CDF collaboration, F. Abe *et al.*, *Observation of the* $\mathrm{B_c}$ *meson in* $\mathrm{p\overline{p}}$ *collisions at* $\sqrt{s} = 1.8$ *TeV*, Phys. Rev. Lett. **81** (1998) 2432, arXiv:hep-ex/9805034.

[23] CDF Collaboration, F. Abe *et al.*, *Observation of* $\mathrm{B_c}$ *mesons in* $\mathrm{p\overline{p}}$ *collisions at* $\sqrt{s} = 1.8$ *TeV*, Phys. Rev. **D58** (1998) 112004, arXiv:hep-ex/9804014.

[24] M. Bauer, B. Stech, and M. Wirbel, *Exclusive non-leptonic decays of* D-, $\mathrm{D_s}$-, *and* B-*mesons*, Z. Phys. **C34** (1987) 103.

[25] M. Wirbel, *Description of weak decays of* D *and* B *mesons*, Prog. Part. Nucl. Phys. **21** (1988) 33.

[26] A. K. Likhoded and A. V. Luchinsky, *Light hadron production in* $\mathrm{B_c} \to \mathrm{J/\psi} + \mathrm{X}$ *decays*, Phys. Rev. **D81** (2010) 014015, arXiv:0910.3089.

[27] A. V. Luchinsky, *Production of* K *mesons in exclusive* $\mathrm{B_c}$ *decays*, arXiv:1307.0953.

[28] A. K. Likhoded and A. V. Luchinsky, *Production of a pion system in exclusive* $\mathrm{B_c} \to \mathrm{V(P)} + \mathrm{n}\pi$ *decays*, Phys. Atom. Nucl. **76** (2013) 787.

[29] LHCb collaboration, A. A. Alves Jr. *et al.*, *The LHCb detector at the LHC*, JINST **3** (2008) S08005.

[30] LHCb collaboration, R. Aaij *et al.*, *LHCb detector performance*, Int. J. Mod. Phys. **A30** (2015) 1530022, arXiv:1412.6352.

[31] R. Aaij *et al.*, *Performance of the LHCb Vertex Locator*, JINST **9** (2014) P09007, arXiv:1405.7808.

[32] R. Arink *et al.*, *Performance of the LHCb Outer Tracker*, JINST **9** (2014) P01002, arXiv:1311.3893.

[33] P. d'Argent *et al.*, *Improved performance of the LHCb Outer Tracker in LHC Run 2*, JINST **12** (2017) P11016, arXiv:1708.00819.

[34] LHCb collaboration, R. Aaij *et al.*, *Measurement of the* Λ_b^0, Ξ_b^-, *and* Ω_b^- *baryon masses*, Phys. Rev. Lett. **110** (2013) 182001, arXiv:1302.1072.

[35] LHCb collaboration, R. Aaij *et al.*, *Precision measurement of* D *meson mass differences*, JHEP **06** (2013) 065, arXiv:1304.6865.

[36] M. Adinolfi *et al.*, *Performance of the LHCb RICH detector at the LHC*, Eur. Phys. J. **C73** (2013) 2431, arXiv:1211.6759.

[37] A. A. Alves Jr. *et al.*, *Performance of the LHCb muon system*, JINST **8** (2013) P02022, arXiv:1211.1346.

[38] R. Aaij *et al.*, *The LHCb trigger and its performance in 2011*, JINST **8** (2013) P04022, arXiv:1211.3055.

[39] T. Sjöstrand, S. Mrenna, and P. Skands, *A brief introduction to* PYTHIA 8.1, Comput. Phys. Commun. **178** (2008) 852, arXiv:0710.3820.

[40] I. Belyaev *et al.*, *Handling of the generation of primary events in* GAUSS*, the LHCb simulation framework*, J. Phys. Conf. Ser. **331** (2011) 032047.

[41] D. J. Lange, *The* EVTGEN *particle decay simulation package*, Nucl. Instrum. Meth. **A462** (2001) 152.

[42] N. Davidson, T. Przedzinski, and Z. Was, *PHOTOS interface in C++: Technical and physics documentation*, Comp. Phys. Comm. **199** (2016) 86, arXiv:1011.0937.

[43] A. V. Berezhnoy, A. K. Likhoded, and A. V. Luchinsky, BC_NPI *module for the analysis of* $B_c \to J/\psi + n\pi$ *and* $B_c \to B_s^0 + n\pi$ *decays within the* EVTGEN *package*, arXiv:1104.0808.

[44] LHCb collaboration, R. Aaij *et al.*, *Observation of* $J/\psi\,\phi$ *structures consistent with exotic states from amplitude analysis of* $B^+ \to J/\psi\,\phi K^+$ *decays*, Phys. Rev. Lett. **118** (2017) 022003, arXiv:1606.07895.

[45] LHCb collaboration, R. Aaij *et al.*, *Amplitude analysis of* $B^+ \to J/\psi\,\phi K^+$ *decays*, Phys. Rev. **D95** (2017) 012002, arXiv:1606.07898.

[46] Geant4 collaboration, J. Allison *et al.*, GEANT4 *developments and applications*, IEEE Trans. Nucl. Sci. **53** (2006) 270; Geant4 collaboration, S. Agostinelli *et al.*, GEANT4 – *a simulation toolkit*, Nucl. Instrum. Meth. **A506** (2003) 250.

[47] M. Clemencic *et al.*, *The LHCb simulation application,* GAUSS*: design, evolution and experience*, J. Phys. Conf. Ser. **331** (2011) 032023.

[48] LHCb collaboration, R. Aaij *et al.*, *Measurement of the track reconstruction efficiency at LHCb*, JINST **10** (2015) P02007, arXiv:1408.1251.

[49] A. Powell *et al.*, *Particle identification at LHCb*, PoS **ICHEP2010** (2010) 020, LHCb-PROC-2011-008.

[50] W. D. Hulsbergen, *Decay chain fitting with a Kalman filter*, Nucl. Instrum. Meth. **A552** (2005) 566, arXiv:physics/0503191.

[51] Particle Data Group, P. A. Zyla *et al.*, *Review of particle physics*, Prog. Theor. Exp. Phys. **2020** (2020) 083C01, and 2021 update.

[52] LHCb collaboration, R. Aaij *et al.*, *Study of the* $\psi_2(3823)$ *and* $\chi_{c1}(3872)$ *states in* $B^+ \to (J/\psi\,\pi^+\pi^-)K^+$ *decays*, JHEP **08** (2020) 123, arXiv:2005.13422.

[53] LHCb collaboration, R. Aaij *et al.*, *Study of* $B_s^0 \to J/\psi\,\pi^+\pi^-K^+K^-$ *decays*, JHEP **02** (2021) 024, arXiv:2011.01867.

[54] LHCb collaboration, R. Aaij *et al.*, *Observation of* J/ψ *-pair production in* pp *collisions at* $\sqrt{s} = 7\,TeV$, Phys. Lett. **B707** (2012) 52, arXiv:1109.0963.

[55] T. Skwarnicki, *A study of the radiative cascade transitions between the* Υ' *and* Υ *resonances*, PhD thesis, Institute of Nuclear Physics, Krakow, 1986, DESY-F31-86-02.

[56] E. Byckling and K. Kajantie, *Particle kinematics*, John Wiley & Sons Inc., New York, 1973.

[57] LHCb collaboration, R. Aaij *et al.*, *Study of the lineshape of the* $\chi_{c1}(3872)$ *state*, Phys. Rev. **D102** (2020) 092005, arXiv:2005.13419.

[58] M. Pivk and F. R. Le Diberder, *sPlot: a statistical tool to unfold data distributions*, Nucl. Instrum. Meth. **A555** (2005) 356, arXiv:physics/0402083.

[59] S. S. Wilks, *The large-sample distribution of the likelihood ratio for testing composite hypotheses*, Ann. Math. Stat. **9** (1938) 60.

[60] CLEO collaboration, D. M. Asner *et al.*, *Hadronic structure in the decay* $\tau^- \to \nu_\tau\pi^-\pi^0\pi^0$ *and the sign of the tau neutrino helicity*, Phys. Rev. **D61** (1999) 012002, arXiv:hep-ex/9902022.

[61] J. M. Blatt and V. F. Weisskopf, *Theoretical nuclear physics*, Springer, New York, 1952.

[62] S. Okubo, ϕ*-meson and unitary symmetry model*, Phys. Lett. **5** (1963) 165.

[63] G. Zweig, *An* SU_3 *model for strong interaction symmetry and its breaking; Version 2* CERN-TH-412, CERN, Geneva, 1964.

[64] J. Iizuka, *A systematics and phenomenology of meson family*, Suppl. Prog. Theor. Phys. **37** (1966) 21.

[65] R. Aaij *et al.*, *Selection and processing of calibration samples to measure the particle identification performance of the LHCb experiment in Run 2*, EPJ Tech. Instrum. **6** (2019) 1, arXiv:1803.00824.

[66] D. Martínez Santos and F. Dupertuis, *Mass distributions marginalized over per-event errors*, Nucl. Instrum. Meth. **A764** (2014) 150, arXiv:1312.5000.

[67] LHCb collaboration, R. Aaij *et al.*, *Measurement of relative branching fractions of* B *decays to* $\psi(2S)$ *and* J/ψ *mesons*, Eur. Phys. J. **C72** (2012) 2118, arXiv:1205.0918.

[68] G. J. Gounaris and J. J. Sakurai, *Finite-width corrections to the vector-meson-dominance prediction for* $\rho^0 \to e^+e^-$, Phys. Rev. Lett. **21** (1968) 244.

[69] LHCb collaboration, R. Aaij *et al.*, *First observation of the decays* $\overline{B}^0 \to D^+K^-\pi^+\pi^-$ *and* $B^- \to D^0K^-\pi^+\pi^-$, Phys. Rev. Lett. **108** (2012) 161801, arXiv:1201.4402.

[70] LHCb collaboration, R. Aaij *et al.*, *Study of* $B^0 \to D^{*-}\pi^+\pi^-\pi^+$ *and* $B^0 \to D^{*-}K^+\pi^-\pi^+$ *decays*, Phys. Rev. **D87** (2013) 092001, arXiv:1303.6861.

[71] LHCb collaboration, R. Aaij *et al.*, *First observation of the decays* $\overline{B}^0_{(s)} \to D_s^+K^-\pi^+\pi^-$ *and* $\overline{B}^0_s \to D_{s1}(2536)^+\pi^-$, Phys. Rev. **D86** (2012) 112005, arXiv:1211.1541.

LHCb collaboration

R. Aaij[32], A.S.W. Abdelmotteleb[56], C. Abellán Beteta[50], F.J. Abudinen Gallego[56], T. Ackernley[60], B. Adeva[46], M. Adinolfi[54], H. Afsharnia[9], C. Agapopoulou[13], C.A. Aidala[87], S. Aiola[25], Z. Ajaltouni[9], S. Akar[65], J. Albrecht[15], F. Alessio[48], M. Alexander[59], A. Alfonso Albero[45], Z. Aliouche[62], G. Alkhazov[38], P. Alvarez Cartelle[55], S. Amato[2], J.L. Amey[54], Y. Amhis[11], L. An[48], L. Anderlini[22], A. Andreianov[38], M. Andreotti[21], F. Archilli[17], A. Artamonov[44], M. Artuso[68], K. Arzymatov[42], E. Aslanides[10], M. Atzeni[50], B. Audurier[12], S. Bachmann[17], M. Bachmayer[49], J.J. Back[56], P. Baladron Rodriguez[46], V. Balagura[12], W. Baldini[21], J. Baptista Leite[1], M. Barbetti[22,h], R.J. Barlow[62], S. Barsuk[11], W. Barter[61], M. Bartolini[24,i], F. Baryshnikov[83], J.M. Basels[14], S. Bashir[34], G. Bassi[29], B. Batsukh[68], A. Battig[15], A. Bay[49], A. Beck[56], M. Becker[15], F. Bedeschi[29], I. Bediaga[1], A. Beiter[68], V. Belavin[42], S. Belin[27], V. Bellee[50], K. Belous[44], I. Belov[40], I. Belyaev[41], G. Bencivenni[23], E. Ben-Haim[13], A. Berezhnoy[40], R. Bernet[50], D. Berninghoff[17], H.C. Bernstein[68], C. Bertella[48], A. Bertolin[28], C. Betancourt[50], F. Betti[48], Ia. Bezshyiko[50], S. Bhasin[54], J. Bhom[35], L. Bian[73], M.S. Bieker[15], S. Bifani[53], P. Billoir[13], A. Biolchini[32], M. Birch[61], F.C.R. Bishop[55], A. Bitadze[62], A. Bizzeti[22,l], M. Bjørn[63], M.P. Blago[48], T. Blake[56], F. Blanc[49], S. Blusk[68], D. Bobulska[59], J.A. Boelhauve[15], O. Boente Garcia[46], T. Boettcher[65], A. Boldyrev[82], A. Bondar[43], N. Bondar[38,48], S. Borghi[62], M. Borisyak[42], M. Borsato[17], J.T. Borsuk[35], S.A. Bouchiba[49], T.J.V. Bowcock[60], A. Boyer[48], C. Bozzi[21], M.J. Bradley[61], S. Braun[66], A. Brea Rodriguez[46], J. Brodzicka[35], A. Brossa Gonzalo[56], D. Brundu[27], A. Buonaura[50], L. Buonincontri[28], A.T. Burke[62], C. Burr[48], A. Bursche[72], A. Butkevich[39], J.S. Butter[32], J. Buytaert[48], W. Byczynski[48], S. Cadeddu[27], H. Cai[73], R. Calabrese[21,g], L. Calefice[15,13], S. Cali[23], R. Calladine[53], M. Calvi[26,k], M. Calvo Gomez[85], P. Camargo Magalhaes[54], P. Campana[23], A.F. Campoverde Quezada[6], S. Capelli[26,k], L. Capriotti[20,e], A. Carbone[20,e], G. Carboni[31,q], R. Cardinale[24,i], A. Cardini[27], I. Carli[4], P. Carniti[26,k], L. Carus[14], K. Carvalho Akiba[32], A. Casais Vidal[46], R. Caspary[17], G. Casse[60], M. Cattaneo[48], G. Cavallero[48], S. Celani[49], J. Cerasoli[10], D. Cervenkov[63], A.J. Chadwick[60], M.G. Chapman[54], M. Charles[13], Ph. Charpentier[48], G. Chatzikonstantinidis[53], C.A. Chavez Barajas[60], M. Chefdeville[8], C. Chen[3], S. Chen[4], A. Chernov[35], V. Chobanova[46], S. Cholak[49], M. Chrzaszcz[35], A. Chubykin[38], V. Chulikov[38], P. Ciambrone[23], M.F. Cicala[56], X. Cid Vidal[46], G. Ciezarek[48], P.E.L. Clarke[58], M. Clemencic[48], H.V. Cliff[55], J. Closier[48], J.L. Cobbledick[62], V. Coco[48], J.A.B. Coelho[11], J. Cogan[10], E. Cogneras[9], L. Cojocariu[37], P. Collins[48], T. Colombo[48], L. Congedo[19,d], A. Contu[27], N. Cooke[53], G. Coombs[59], I. Corredoira [46], G. Corti[48], C.M. Costa Sobral[56], B. Couturier[48], D.C. Craik[64], J. Crkovská[67], M. Cruz Torres[1], R. Currie[58], C.L. Da Silva[67], S. Dadabaev[83], L. Dai[71], E. Dall'Occo[15], J. Dalseno[46], C. D'Ambrosio[48], A. Danilina[41], P. d'Argent[48], A. Dashkina[83], J.E. Davies[62], A. Davis[62], O. De Aguiar Francisco[62], K. De Bruyn[79], S. De Capua[62], M. De Cian[49], E. De Lucia[23], J.M. De Miranda[1], L. De Paula[2], M. De Serio[19,d], D. De Simone[50], P. De Simone[23], F. De Vellis[15], J.A. de Vries[80], C.T. Dean[67], F. Debernardis[19,d], D. Decamp[8], V. Dedu[10], L. Del Buono[13], B. Delaney[55], H.-P. Dembinski[15], A. Dendek[34], V. Denysenko[50], D. Derkach[82], O. Deschamps[9], F. Desse[11], F. Dettori[27,f], B. Dey[77], A. Di Cicco[23], P. Di Nezza[23], S. Didenko[83], L. Dieste Maronas[46], H. Dijkstra[48], V. Dobishuk[52], C. Dong[3], A.M. Donohoe[18], F. Dordei[27], A.C. dos Reis[1], L. Douglas[59], A. Dovbnya[51], A.G. Downes[8], M.W. Dudek[35], L. Dufour[48], V. Duk[78], P. Durante[48], J.M. Durham[67], D. Dutta[62], A. Dziurda[35], A. Dzyuba[38], S. Easo[57], U. Egede[69], A. Egorychev[41], V. Egorychev[41], S. Eidelman[43,v,†], S. Eisenhardt[58], S. Ek-In[49], L. Eklund[86], S. Ely[68], A. Ene[37], E. Epple[67], S. Escher[14], J. Eschle[50], S. Esen[13], T. Evans[48], Y. Fan[6], B. Fang[73], S. Farry[60], D. Fazzini[26,k], M. Féo[48], A. Fernandez Prieto[46], A.D. Fernez[66], F. Ferrari[20,e], L. Ferreira Lopes[49], F. Ferreira Rodrigues[2], S. Ferreres Sole[32], M. Ferrillo[50], M. Ferro-Luzzi[48], S. Filippov[39], R.A. Fini[19], M. Fiorini[21,g],

M. Firlej[34], K.M. Fischer[63], D.S. Fitzgerald[87], C. Fitzpatrick[62], T. Fiutowski[34], A. Fkiaras[48], F. Fleuret[12], M. Fontana[13], F. Fontanelli[24,i], R. Forty[48], D. Foulds-Holt[55], V. Franco Lima[60], M. Franco Sevilla[66], M. Frank[48], E. Franzoso[21], G. Frau[17], C. Frei[48], D.A. Friday[59], J. Fu[6], Q. Fuehring[15], E. Gabriel[32], G. Galati[19,d], A. Gallas Torreira[46], D. Galli[20,e], S. Gambetta[58,48], Y. Gan[3], M. Gandelman[2], P. Gandini[25], Y. Gao[5], M. Garau[27], L.M. Garcia Martin[56], P. Garcia Moreno[45], J. García Pardiñas[26,k], B. Garcia Plana[46], F.A. Garcia Rosales[12], L. Garrido[45], C. Gaspar[48], R.E. Geertsema[32], D. Gerick[17], L.L. Gerken[15], E. Gersabeck[62], M. Gersabeck[62], T. Gershon[56], D. Gerstel[10], L. Giambastiani[28], V. Gibson[55], H.K. Giemza[36], A.L. Gilman[63], M. Giovannetti[23,q], A. Gioventù[46], P. Gironella Gironell[45], C. Giugliano[21,g,48], K. Gizdov[58], E.L. Gkougkousis[48], V.V. Gligorov[13], C. Göbel[70], E. Golobardes[85], D. Golubkov[41], A. Golutvin[61,83], A. Gomes[1,a], S. Gomez Fernandez[45], F. Goncalves Abrantes[63], M. Goncerz[35], G. Gong[3], P. Gorbounov[41], I.V. Gorelov[40], C. Gotti[26], E. Govorkova[48], J.P. Grabowski[17], T. Grammatico[13], L.A. Granado Cardoso[48], E. Graugés[45], E. Graverini[49], G. Graziani[22], A. Grecu[37], L.M. Greeven[32], N.A. Grieser[4], L. Grillo[62], S. Gromov[83], B.R. Gruberg Cazon[63], C. Gu[3], M. Guarise[21], M. Guittiere[11], P. A. Günther[17], E. Gushchin[39], A. Guth[14], Y. Guz[44], T. Gys[48], T. Hadavizadeh[69], G. Haefeli[49], C. Haen[48], J. Haimberger[48], T. Halewood-leagas[60], P.M. Hamilton[66], J.P. Hammerich[60], Q. Han[7], X. Han[17], T.H. Hancock[63], E.B. Hansen[62], S. Hansmann-Menzemer[17], N. Harnew[63], T. Harrison[60], C. Hasse[48], M. Hatch[48], J. He[6,b], M. Hecker[61], K. Heijhoff[32], K. Heinicke[15], R.D.L. Henderson[69], A.M. Hennequin[48], K. Hennessy[60], L. Henry[48], J. Heuel[14], A. Hicheur[2], D. Hill[49], M. Hilton[62], S.E. Hollitt[15], R. Hou[7], Y. Hou[8], J. Hu[17], J. Hu[72], W. Hu[7], X. Hu[3], W. Huang[6], X. Huang[73], W. Hulsbergen[32], R.J. Hunter[56], M. Hushchyn[82], D. Hutchcroft[60], D. Hynds[32], P. Ibis[15], M. Idzik[34], D. Ilin[38], P. Ilten[65], A. Inglessi[38], A. Ishteev[83], K. Ivshin[38], R. Jacobsson[48], H. Jage[14], S. Jakobsen[48], E. Jans[32], B.K. Jashal[47], A. Jawahery[66], V. Jevtic[15], X. Jiang[4], M. John[63], D. Johnson[64], C.R. Jones[55], T.P. Jones[56], B. Jost[48], N. Jurik[48], S.H. Kalavan Kadavath[34], S. Kandybei[51], Y. Kang[3], M. Karacson[48], M. Karpov[82], F. Keizer[48], D.M. Keller[68], M. Kenzie[56], T. Ketel[33], B. Khanji[15], A. Kharisova[84], S. Kholodenko[44], T. Kirn[14], V.S. Kirsebom[49], O. Kitouni[64], S. Klaver[32], N. Kleijne[29], K. Klimaszewski[36], M.R. Kmiec[36], S. Koliiev[52], A. Kondybayeva[83], A. Konoplyannikov[41], P. Kopciewicz[34], R. Kopecna[17], P. Koppenburg[32], M. Korolev[40], I. Kostiuk[32,52], O. Kot[52], S. Kotriakhova[21,38], P. Kravchenko[38], L. Kravchuk[39], R.D. Krawczyk[48], M. Kreps[56], F. Kress[61], S. Kretzschmar[14], P. Krokovny[43,v], W. Krupa[34], W. Krzemien[36], J. Kubat[17], M. Kucharczyk[35], V. Kudryavtsev[43,v], H.S. Kuindersma[32,33], G.J. Kunde[67], T. Kvaratskheliya[41], D. Lacarrere[48], G. Lafferty[62], A. Lai[27], A. Lampis[27], D. Lancierini[50], J.J. Lane[62], R. Lane[54], G. Lanfranchi[23], C. Langenbruch[14], J. Langer[15], O. Lantwin[83], T. Latham[56], F. Lazzari[29,r], R. Le Gac[10], S.H. Lee[87], R. Lefèvre[9], A. Leflat[40], S. Legotin[83], O. Leroy[10], T. Lesiak[35], B. Leverington[17], H. Li[72], P. Li[17], S. Li[7], Y. Li[4], Y. Li[4], Z. Li[68], X. Liang[68], T. Lin[61], R. Lindner[48], V. Lisovskyi[15], R. Litvinov[27], G. Liu[72], H. Liu[6], Q. Liu[6], S. Liu[4], A. Lobo Salvia[45], A. Loi[27], J. Lomba Castro[46], I. Longstaff[59], J.H. Lopes[2], S. Lopez Solino[46], G.H. Lovell[55], Y. Lu[4], C. Lucarelli[22,h], D. Lucchesi[28,m], S. Luchuk[39], M. Lucio Martinez[32], V. Lukashenko[32,52], Y. Luo[3], A. Lupato[62], E. Luppi[21,g], O. Lupton[56], A. Lusiani[29,n], X. Lyu[6], L. Ma[4], R. Ma[6], S. Maccolini[20,e], F. Machefert[11], F. Maciuc[37], V. Macko[49], P. Mackowiak[15], S. Maddrell-Mander[54], O. Madejczyk[34], L.R. Madhan Mohan[54], O. Maev[38], A. Maevskiy[82], D. Maisuzenko[38], M.W. Majewski[34], J.J. Malczewski[35], S. Malde[63], B. Malecki[48], A. Malinin[81], T. Maltsev[43,v], H. Malygina[17], G. Manca[27,f], G. Mancinelli[10], D. Manuzzi[20,e], D. Marangotto[25,j], J. Maratas[9,t], J.F. Marchand[8], U. Marconi[20], S. Mariani[22,h], C. Marin Benito[48], M. Marinangeli[49], J. Marks[17], A.M. Marshall[54], P.J. Marshall[60], G. Martelli[78], G. Martellotti[30], L. Martinazzoli[48,k], M. Martinelli[26,k], D. Martinez Santos[46], F. Martinez Vidal[47], A. Massafferri[1], M. Materok[14], R. Matev[48], A. Mathad[50], V. Matiunin[41], C. Matteuzzi[26], K.R. Mattioli[87], A. Mauri[32], E. Maurice[12], J. Mauricio[45], M. Mazurek[48], M. McCann[61], L. Mcconnell[18], T.H. Mcgrath[62], N.T. Mchugh[59], A. McNab[62], R. McNulty[18],

J.V. Mead[60], B. Meadows[65], G. Meier[15], N. Meinert[76], D. Melnychuk[36], S. Meloni[26,k], M. Merk[32,80], A. Merli[25,j], L. Meyer Garcia[2], M. Mikhasenko[75,c], D.A. Milanes[74], E. Millard[56], M. Milovanovic[48], M.-N. Minard[8], A. Minotti[26,k], L. Minzoni[21,g], S.E. Mitchell[58], B. Mitreska[62], D.S. Mitzel[15], A. Mödden [15], R.A. Mohammed[63], R.D. Moise[61], S. Mokhnenko[82], T. Mombächer[46], I.A. Monroy[74], S. Monteil[9], M. Morandin[28], G. Morello[23], M.J. Morello[29,n], J. Moron[34], A.B. Morris[75], A.G. Morris[56], R. Mountain[68], H. Mu[3], F. Muheim[58,48], M. Mulder[48], D. Müller[48], K. Müller[50], C.H. Murphy[63], D. Murray[62], R. Murta[61], P. Muzzetto[27,48], P. Naik[54], T. Nakada[49], R. Nandakumar[57], T. Nanut[49], I. Nasteva[2], M. Needham[58], N. Neri[25,j], S. Neubert[75], N. Neufeld[48], R. Newcombe[61], E.M. Niel[11], S. Nieswand[14], N. Nikitin[40], N.S. Nolte[64], C. Normand[8], C. Nunez[87], A. Oblakowska-Mucha[34], V. Obraztsov[44], T. Oeser[14], D.P. O'Hanlon[54], S. Okamura[21], R. Oldeman[27,f], F. Oliva[58], M.E. Olivares[68], C.J.G. Onderwater[79], R.H. O'Neil[58], J.M. Otalora Goicochea[2], T. Ovsiannikova[41], P. Owen[50], A. Oyanguren[47], K.O. Padeken[75], B. Pagare[56], P.R. Pais[48], T. Pajero[63], A. Palano[19], M. Palutan[23], Y. Pan[62], G. Panshin[84], A. Papanestis[57], M. Pappagallo[19,d], L.L. Pappalardo[21,g], C. Pappenheimer[65], W. Parker[66], C. Parkes[62], B. Passalacqua[21], G. Passaleva[22], A. Pastore[19], M. Patel[61], C. Patrignani[20,e], C.J. Pawley[80], A. Pearce[48,57], A. Pellegrino[32], M. Pepe Altarelli[48], S. Perazzini[20], D. Pereima[41], A. Pereiro Castro[46], P. Perret[9], M. Petric[59,48], K. Petridis[54], A. Petrolini[24,i], A. Petrov[81], S. Petrucci[58], M. Petruzzo[25], T.T.H. Pham[68], A. Philippov[42], L. Pica[29,n], M. Piccini[78], B. Pietrzyk[8], G. Pietrzyk[49], M. Pili[63], D. Pinci[30], F. Pisani[48], M. Pizzichemi[26,48,k], Resmi P.K[10], V. Placinta[37], J. Plews[53], M. Plo Casasus[46], F. Polci[13], M. Poli Lener[23], M. Poliakova[68], A. Poluektov[10], N. Polukhina[83,u], I. Polyakov[68], E. Polycarpo[2], S. Ponce[48], D. Popov[6,48], S. Popov[42], S. Poslavskii[44], K. Prasanth[35], L. Promberger[48], C. Prouve[46], V. Pugatch[52], V. Puill[11], H. Pullen[63], G. Punzi[29,o], H. Qi[3], W. Qian[6], J. Qin[6], N. Qin[3], R. Quagliani[49], B. Quintana[8], N.V. Raab[18], R.I. Rabadan Trejo[6], B. Rachwal[34], J.H. Rademacker[54], M. Rama[29], M. Ramos Pernas[56], M.S. Rangel[2], F. Ratnikov[42,82], G. Raven[33], M. Reboud[8], F. Redi[49], F. Reiss[62], C. Remon Alepuz[47], Z. Ren[3], V. Renaudin[63], R. Ribatti[29], S. Ricciardi[57], K. Rinnert[60], P. Robbe[11], G. Robertson[58], A.B. Rodrigues[49], E. Rodrigues[60], J.A. Rodriguez Lopez[74], E.R.R. Rodriguez Rodriguez[46], A. Rollings[63], P. Roloff[48], V. Romanovskiy[44], M. Romero Lamas[46], A. Romero Vidal[46], J.D. Roth[87], M. Rotondo[23], M.S. Rudolph[68], T. Ruf[48], R.A. Ruiz Fernandez[46], J. Ruiz Vidal[47], A. Ryzhikov[82], J. Ryzka[34], J.J. Saborido Silva[46], N. Sagidova[38], N. Sahoo[56], B. Saitta[27,f], M. Salomoni[48], C. Sanchez Gras[32], R. Santacesaria[30], C. Santamarina Rios[46], M. Santimaria[23], E. Santovetti[31,q], D. Saranin[83], G. Sarpis[14], M. Sarpis[75], A. Sarti[30], C. Satriano[30,p], A. Satta[31], M. Saur[15], D. Savrina[41,40], H. Sazak[9], L.G. Scantlebury Smead[63], A. Scarabotto[13], S. Schael[14], S. Scherl[60], M. Schiller[59], H. Schindler[48], M. Schmelling[16], B. Schmidt[48], S. Schmitt[14], O. Schneider[49], A. Schopper[48], M. Schubiger[32], S. Schulte[49], M.H. Schune[11], R. Schwemmer[48], B. Sciascia[23,48], S. Sellam[46], A. Semennikov[41], M. Senghi Soares[33], A. Sergi[24,i], N. Serra[50], L. Sestini[28], A. Seuthe[15], Y. Shang[5], D.M. Shangase[87], M. Shapkin[44], I. Shchemerov[83], L. Shchutska[49], T. Shears[60], L. Shekhtman[43,v], Z. Shen[5], S. Sheng[4], V. Shevchenko[81], E.B. Shields[26,k], Y. Shimizu[11], E. Shmanin[83], J.D. Shupperd[68], B.G. Siddi[21], R. Silva Coutinho[50], G. Simi[28], S. Simone[19,d], N. Skidmore[62], T. Skwarnicki[68], M.W. Slater[53], I. Slazyk[21,g], J.C. Smallwood[63], J.G. Smeaton[55], A. Smetkina[41], E. Smith[50], M. Smith[61], A. Snoch[32], L. Soares Lavra[9], M.D. Sokoloff[65], F.J.P. Soler[59], A. Solovev[38], I. Solovyev[38], F.L. Souza De Almeida[2], B. Souza De Paula[2], B. Spaan[15], E. Spadaro Norella[25,j], P. Spradlin[59], F. Stagni[48], M. Stahl[65], S. Stahl[48], S. Stanislaus[63], O. Steinkamp[50,83], O. Stenyakin[44], H. Stevens[15], S. Stone[68], D. Strekalina[83], F. Suljik[63], J. Sun[27], L. Sun[73], Y. Sun[66], P. Svihra[62], P.N. Swallow[53], K. Swientek[34], A. Szabelski[36], T. Szumlak[34], M. Szymanski[48], S. Taneja[62], A.R. Tanner[54], M.D. Tat[63], A. Terentev[83], F. Teubert[48], E. Thomas[48], D.J.D. Thompson[53], K.A. Thomson[60], H. Tilquin[61], V. Tisserand[9], S. T'Jampens[8], M. Tobin[4], L. Tomassetti[21,g],

X. Tong[5], D. Torres Machado[1], D.Y. Tou[13], E. Trifonova[83], C. Trippl[49], G. Tuci[6], A. Tully[49], N. Tuning[32,48], A. Ukleja[36], D.J. Unverzagt[17], E. Ursov[83], A. Usachov[32], A. Ustyuzhanin[42,82], U. Uwer[17], A. Vagner[84], V. Vagnoni[20], A. Valassi[48], G. Valenti[20], N. Valls Canudas[85], M. van Beuzekom[32], M. Van Dijk[49], H. Van Hecke[67], E. van Herwijnen[83], M. van Veghel[79], R. Vazquez Gomez[45], P. Vazquez Regueiro[46], C. Vázquez Sierra[48], S. Vecchi[21], J.J. Velthuis[54], M. Veltri[22,s], A. Venkateswaran[68], M. Veronesi[32], M. Vesterinen[56], D. Vieira[65], M. Vieites Diaz[49], H. Viemann[76], X. Vilasis-Cardona[85], E. Vilella Figueras[60], A. Villa[20], P. Vincent[13], F.C. Volle[11], D. Vom Bruch[10], A. Vorobyev[38], V. Vorobyev[43,v], N. Voropaev[38], K. Vos[80], R. Waldi[17], J. Walsh[29], C. Wang[17], J. Wang[5], J. Wang[4], J. Wang[3], J. Wang[73], M. Wang[3], R. Wang[54], Y. Wang[7], Z. Wang[50], Z. Wang[3], Z. Wang[6], J.A. Ward[56], N.K. Watson[53], S.G. Weber[13], D. Websdale[61], C. Weisser[64], B.D.C. Westhenry[54], D.J. White[62], M. Whitehead[54], A.R. Wiederhold[56], D. Wiedner[15], G. Wilkinson[63], M. Wilkinson[68], I. Williams[55], M. Williams[64], M.R.J. Williams[58], F.F. Wilson[57], W. Wislicki[36], M. Witek[35], L. Witola[17], G. Wormser[11], S.A. Wotton[55], H. Wu[68], K. Wyllie[48], Z. Xiang[6], D. Xiao[7], Y. Xie[7], A. Xu[5], J. Xu[6], L. Xu[3], M. Xu[7], Q. Xu[6], Z. Xu[5], Z. Xu[6], D. Yang[3], S. Yang[6], Y. Yang[6], Z. Yang[5], Z. Yang[66], Y. Yao[68], L.E. Yeomans[60], H. Yin[7], J. Yu[71], X. Yuan[68], O. Yushchenko[44], E. Zaffaroni[49], M. Zavertyaev[16,u], M. Zdybal[35], O. Zenaiev[48], M. Zeng[3], D. Zhang[7], L. Zhang[3], S. Zhang[71], S. Zhang[5], Y. Zhang[5], Y. Zhang[63], A. Zharkova[83], A. Zhelezov[17], Y. Zheng[6], T. Zhou[5], X. Zhou[6], Y. Zhou[6], V. Zhovkovska[11], X. Zhu[3], X. Zhu[7], Z. Zhu[6], V. Zhukov[14,40], J.B. Zonneveld[58], Q. Zou[4], S. Zucchelli[20,e], D. Zuliani[28], G. Zunica[62].

[1] *Centro Brasileiro de Pesquisas Físicas (CBPF), Rio de Janeiro, Brazil*
[2] *Universidade Federal do Rio de Janeiro (UFRJ), Rio de Janeiro, Brazil*
[3] *Center for High Energy Physics, Tsinghua University, Beijing, China*
[4] *Institute Of High Energy Physics (IHEP), Beijing, China*
[5] *School of Physics State Key Laboratory of Nuclear Physics and Technology, Peking University, Beijing, China*
[6] *University of Chinese Academy of Sciences, Beijing, China*
[7] *Institute of Particle Physics, Central China Normal University, Wuhan, Hubei, China*
[8] *Univ. Savoie Mont Blanc, CNRS, IN2P3-LAPP, Annecy, France*
[9] *Université Clermont Auvergne, CNRS/IN2P3, LPC, Clermont-Ferrand, France*
[10] *Aix Marseille Univ, CNRS/IN2P3, CPPM, Marseille, France*
[11] *Université Paris-Saclay, CNRS/IN2P3, IJCLab, Orsay, France*
[12] *Laboratoire Leprince-Ringuet, CNRS/IN2P3, Ecole Polytechnique, Institut Polytechnique de Paris, Palaiseau, France*
[13] *LPNHE, Sorbonne Université, Paris Diderot Sorbonne Paris Cité, CNRS/IN2P3, Paris, France*
[14] *I. Physikalisches Institut, RWTH Aachen University, Aachen, Germany*
[15] *Fakultät Physik, Technische Universität Dortmund, Dortmund, Germany*
[16] *Max-Planck-Institut für Kernphysik (MPIK), Heidelberg, Germany*
[17] *Physikalisches Institut, Ruprecht-Karls-Universität Heidelberg, Heidelberg, Germany*
[18] *School of Physics, University College Dublin, Dublin, Ireland*
[19] *INFN Sezione di Bari, Bari, Italy*
[20] *INFN Sezione di Bologna, Bologna, Italy*
[21] *INFN Sezione di Ferrara, Ferrara, Italy*
[22] *INFN Sezione di Firenze, Firenze, Italy*
[23] *INFN Laboratori Nazionali di Frascati, Frascati, Italy*
[24] *INFN Sezione di Genova, Genova, Italy*
[25] *INFN Sezione di Milano, Milano, Italy*
[26] *INFN Sezione di Milano-Bicocca, Milano, Italy*
[27] *INFN Sezione di Cagliari, Monserrato, Italy*
[28] *Universita degli Studi di Padova, Universita e INFN, Padova, Padova, Italy*
[29] *INFN Sezione di Pisa, Pisa, Italy*
[30] *INFN Sezione di Roma La Sapienza, Roma, Italy*
[31] *INFN Sezione di Roma Tor Vergata, Roma, Italy*

[32] *Nikhef National Institute for Subatomic Physics, Amsterdam, Netherlands*
[33] *Nikhef National Institute for Subatomic Physics and VU University Amsterdam, Amsterdam, Netherlands*
[34] *AGH - University of Science and Technology, Faculty of Physics and Applied Computer Science, Kraków, Poland*
[35] *Henryk Niewodniczanski Institute of Nuclear Physics Polish Academy of Sciences, Kraków, Poland*
[36] *National Center for Nuclear Research (NCBJ), Warsaw, Poland*
[37] *Horia Hulubei National Institute of Physics and Nuclear Engineering, Bucharest-Magurele, Romania*
[38] *Petersburg Nuclear Physics Institute NRC Kurchatov Institute (PNPI NRC KI), Gatchina, Russia*
[39] *Institute for Nuclear Research of the Russian Academy of Sciences (INR RAS), Moscow, Russia*
[40] *Institute of Nuclear Physics, Moscow State University (SINP MSU), Moscow, Russia*
[41] *Institute of Theoretical and Experimental Physics NRC Kurchatov Institute (ITEP NRC KI), Moscow, Russia*
[42] *Yandex School of Data Analysis, Moscow, Russia*
[43] *Budker Institute of Nuclear Physics (SB RAS), Novosibirsk, Russia*
[44] *Institute for High Energy Physics NRC Kurchatov Institute (IHEP NRC KI), Protvino, Russia, Protvino, Russia*
[45] *ICCUB, Universitat de Barcelona, Barcelona, Spain*
[46] *Instituto Galego de Física de Altas Enerxías (IGFAE), Universidade de Santiago de Compostela, Santiago de Compostela, Spain*
[47] *Instituto de Fisica Corpuscular, Centro Mixto Universidad de Valencia - CSIC, Valencia, Spain*
[48] *European Organization for Nuclear Research (CERN), Geneva, Switzerland*
[49] *Institute of Physics, Ecole Polytechnique Fédérale de Lausanne (EPFL), Lausanne, Switzerland*
[50] *Physik-Institut, Universität Zürich, Zürich, Switzerland*
[51] *NSC Kharkiv Institute of Physics and Technology (NSC KIPT), Kharkiv, Ukraine*
[52] *Institute for Nuclear Research of the National Academy of Sciences (KINR), Kyiv, Ukraine*
[53] *University of Birmingham, Birmingham, United Kingdom*
[54] *H.H. Wills Physics Laboratory, University of Bristol, Bristol, United Kingdom*
[55] *Cavendish Laboratory, University of Cambridge, Cambridge, United Kingdom*
[56] *Department of Physics, University of Warwick, Coventry, United Kingdom*
[57] *STFC Rutherford Appleton Laboratory, Didcot, United Kingdom*
[58] *School of Physics and Astronomy, University of Edinburgh, Edinburgh, United Kingdom*
[59] *School of Physics and Astronomy, University of Glasgow, Glasgow, United Kingdom*
[60] *Oliver Lodge Laboratory, University of Liverpool, Liverpool, United Kingdom*
[61] *Imperial College London, London, United Kingdom*
[62] *Department of Physics and Astronomy, University of Manchester, Manchester, United Kingdom*
[63] *Department of Physics, University of Oxford, Oxford, United Kingdom*
[64] *Massachusetts Institute of Technology, Cambridge, MA, United States*
[65] *University of Cincinnati, Cincinnati, OH, United States*
[66] *University of Maryland, College Park, MD, United States*
[67] *Los Alamos National Laboratory (LANL), Los Alamos, United States*
[68] *Syracuse University, Syracuse, NY, United States*
[69] *School of Physics and Astronomy, Monash University, Melbourne, Australia, associated to* [56]
[70] *Pontifícia Universidade Católica do Rio de Janeiro (PUC-Rio), Rio de Janeiro, Brazil, associated to* [2]
[71] *Physics and Micro Electronic College, Hunan University, Changsha City, China, associated to* [7]
[72] *Guangdong Provincial Key Laboratory of Nuclear Science, Guangdong-Hong Kong Joint Laboratory of Quantum Matter, Institute of Quantum Matter, South China Normal University, Guangzhou, China, associated to* [3]
[73] *School of Physics and Technology, Wuhan University, Wuhan, China, associated to* [3]
[74] *Departamento de Fisica , Universidad Nacional de Colombia, Bogota, Colombia, associated to* [13]
[75] *Universität Bonn - Helmholtz-Institut für Strahlen und Kernphysik, Bonn, Germany, associated to* [17]
[76] *Institut für Physik, Universität Rostock, Rostock, Germany, associated to* [17]
[77] *Eotvos Lorand University, Budapest, Hungary, associated to* [48]
[78] *INFN Sezione di Perugia, Perugia, Italy, associated to* [21]
[79] *Van Swinderen Institute, University of Groningen, Groningen, Netherlands, associated to* [32]
[80] *Universiteit Maastricht, Maastricht, Netherlands, associated to* [32]

[81] *National Research Centre Kurchatov Institute, Moscow, Russia, associated to* [41]
[82] *National Research University Higher School of Economics, Moscow, Russia, associated to* [42]
[83] *National University of Science and Technology "MISIS", Moscow, Russia, associated to* [41]
[84] *National Research Tomsk Polytechnic University, Tomsk, Russia, associated to* [41]
[85] *DS4DS, La Salle, Universitat Ramon Llull, Barcelona, Spain, associated to* [45]
[86] *Department of Physics and Astronomy, Uppsala University, Uppsala, Sweden, associated to* [59]
[87] *University of Michigan, Ann Arbor, United States, associated to* [68]

[a] *Universidade Federal do Triângulo Mineiro (UFTM), Uberaba-MG, Brazil*
[b] *Hangzhou Institute for Advanced Study, UCAS, Hangzhou, China*
[c] *Excellence Cluster ORIGINS, Munich, Germany*
[d] *Università di Bari, Bari, Italy*
[e] *Università di Bologna, Bologna, Italy*
[f] *Università di Cagliari, Cagliari, Italy*
[g] *Università di Ferrara, Ferrara, Italy*
[h] *Università di Firenze, Firenze, Italy*
[i] *Università di Genova, Genova, Italy*
[j] *Università degli Studi di Milano, Milano, Italy*
[k] *Università di Milano Bicocca, Milano, Italy*
[l] *Università di Modena e Reggio Emilia, Modena, Italy*
[m] *Università di Padova, Padova, Italy*
[n] *Scuola Normale Superiore, Pisa, Italy*
[o] *Università di Pisa, Pisa, Italy*
[p] *Università della Basilicata, Potenza, Italy*
[q] *Università di Roma Tor Vergata, Roma, Italy*
[r] *Università di Siena, Siena, Italy*
[s] *Università di Urbino, Urbino, Italy*
[t] *MSU - Iligan Institute of Technology (MSU-IIT), Iligan, Philippines*
[u] *P.N. Lebedev Physical Institute, Russian Academy of Science (LPI RAS), Moscow, Russia*
[v] *Novosibirsk State University, Novosibirsk, Russia*

[†] *Deceased*